Impacts of diversity in commercial building occupancy profiles on district energy demand and supply

Working Paper

Author(s):
Happle, Gabriel; Fonseca, Jimeno A.; Schlueter, Arno

Publication date:
2020

Permanent link:
https://doi.org/10.3929/ethz-b-000407103

Impacts of diversity in commercial building occupancy profiles on district energy demand and supply

Gabriel Happle[a,b,], Jimeno A. Fonseca[a,b], Arno Schlueter[a,b]

[a]*Future Cities Laboratory, Singapore-ETH Centre, 1 Create Way, CREATE Tower, Singapore 138602*
[b]*Architecture and Building Systems, Institute of Technology in Architecture, ETH Zurich, Stefano-Franscini-Platz 1, CH-8093 Zurich, Switzerland*

Abstract

Urban building energy models (UBEM) have the potential to become integral planning tools for district energy systems due to the dynamic, interactive and complex nature of temporal building energy demand patterns. Although the demand patterns are related to the occupancy profiles of buildings supplied by district energy systems, occupant behavior in current UBEM approaches does not usually consider *diversity in occupancy profiles* among buildings of the same use-type.

In this work, a novel method to create context-specific, data-driven commercial building occupancy profiles was used to generate, *diverse* and *non-diverse* urban building occupant presence models (UBOP). *Diverse* UBOP randomly assigned occupancy profiles to buildings. *Non-diverse* UBOP assigned the data-driven mean or median profile to all buildings. ASHRAE standard profiles and occupant densities served as a baseline for comparison.

The impact of *diverse* vs. *non-diverse* UBOP was assessed by comparing UBEM simulations for district energy efficiency benchmarking, renewable energy integration potential, and district energy system design, using a case study in Singapore. The results demonstrate that, because of the relationship between occupant presence and building systems operation, occupancy profiles are highly sensitive parameters for district energy demand predictions. For the case study, the energy demand estimation is significantly influenced by the shape of occupancy profiles. In particular, the choice of UBOP influences the cooling demand to the degree that district cooling system design

Email address: `happle@arch.ethz.ch` (Gabriel Happle)

decisions might be impacted. Therefore, it is advisable to use *diverse* UBOP and to run probabilistic UBEM simulations for district energy system design.

Keywords: Urban building energy model, energy-related occupant behavior, data-driven urban building occupant presence model, district energy system

1. Introduction

1.1. Urban Building Energy Models and Occupant Behavior

Urban building energy models (UBEM) [1] have the potential to become integral planning tools for urban design and district energy systems [2, 3]. The first step of such bottom-up, physics-based models is the prediction of the dynamic energy demands of individual buildings in the district. This energy demand prediction is dependent on the various modeling assumptions related to building physics, building systems, and energy-related occupant behavior, which are sensitive [4, 5, 6]. Due to this sensitivity, it is still unclear to what extent and for what exact purposes UBEM will be suitable decision-making tools for urban design and infrastructure planning. One purpose of UBEM could be the planning of district heating systems (DHS) and district cooling systems (DCS).

One main argument for DHS and DCS is the reduction in capital cost due to the *load diversity*, which "can substantially reduce the total equipment capacity requirement" [7]. What this means is that the "total heating and cooling capacities do not need to be as large as the sum of capacities that would occur in individual buildings, because peak demands will not all occur at the same time" [8]. This effect has to do with the diversity of building geometries, construction properties, and building use-types within a district. This diversity leads to differences in the temporal energy demand patterns of buildings, which can also be beneficial for achieving renewable energy supply targets in the district [9]. Current UBEM approaches are able to consider differences in geometry and construction. However, they mostly rely on standard assumptions regarding the occupant behavior of specific building use-types, which are then applied for all buildings of the same use-type [10]. The usual approach for urban building occupant presence modeling (UBOP) consists of typical occupant density values and relative occupancy profiles, which are multiplied with the buildings' floor area to obtain the number of people present at any given hour of the year. Such typical values are published by professional associations like the American Society of Heating, Refrigerating and Air-Conditioning Engineers (ASHRAE) for example [11, 12] or the Swiss Society of Engineers and Architects (SIA) [13]. While these approaches consider differences *between use-types*, the variability *within use-types* is often neglected. This simplification could affect the UBEM simulation results, especially in mixed-use districts with a considerable share of commercial buildings. Such buildings, for example restaurants and retail buildings, can have highly variable occupancy profiles.

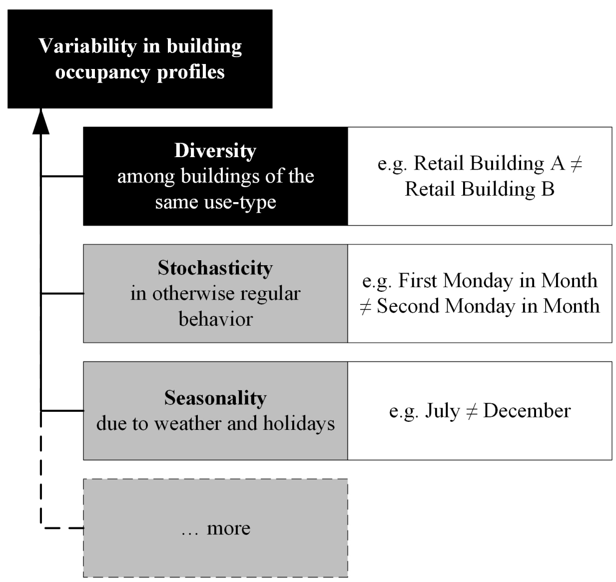

Figure 1: Possible causes and examples of variability in building occupancy profiles on the district and urban scale.

Fig. 1 introduces some of the causes that could lead to variability in occupancy profiles within buildings of the same use-type. We use the terminology *diversity*, *stochasticity*, and *seasonality* to describe them. Diversity is used to describe fundamental differences between buildings of the same use-type. E.g., a clothing store vs. a grocery store or a fast-food restaurant vs. a fine dining restaurant. Stochasticity is used to describe the random variations in regular daily profiles of a specific building. E.g., the timing and height of the regular Monday lunchtime peak in a restaurant might vary randomly from week to week within certain bounds. Finally, seasonality is used to describe underlying behavioral trends influencing all types of buildings, such as the weather or holidays. E.g., people might generally spend more time outdoors during pleasant weather, which might reduce the overall occupancy of shopping malls. Diversity was selected as the focus of this work because to date, 1) this critical aspect has not been addressed in the literature, and 2) because commercial building occupancy profiles with 'real' observed diversity can be collected to provide novel insight into district energy systems [14].

In the next section, existing modeling approaches dealing with variability in occupancy profiles on the district- and urban-scales are introduced. On the building-scale, occupant behaviour is extensively studied in the context of the International Energy Agency (IEA) Annex 66 [15] and its follow-up Annex 79 [16] that is working on "dynamic, stochastic, agent-based, and data-driven" occupant models [17].

1.2. Advanced Urban-Scale Occupant Behavior Models

Currently, there are few publications focused on advanced occupant behavior modeling approaches in district or urban energy simulations [10]. So far, approaches that consider stochasticity and/or diversity in occupant presence profiles focused on mono-functional residential [18, 19, 20, 21, 22, 23, 24, 25, 26] or office [27, 28, 29, 30] districts and are mostly based on building-scale approaches, which are in turn based on residential time-use survey (TUS) data, e.g. [31], or observed data in offices, e.g. [32].Additionally more recently, novel approaches that couple urban mobility models with UBEM have been addressed in the literature [33]. For more detail on the previously mentioned approaches, please refer to the literature review by Happle et al. [10] .

In the following subsections, advanced approaches for UBOP that consider stochasticity and/or diversity are introduced, and the categories of *space-based* and *person-based* approaches from [10] are used to describe them. To our knowledge, the only approach that considers seasonality is the SIA standard that contains monthly multiplication factors to adjust the occupancy profiles throughout the year [13].

1.2.1. Space-based approaches that add stochasticity to regular profiles

Stochasticity can be added to otherwise regular profiles with the concept of Monte-Carlo Markov-Chains (MCMC), as proposed by Page et al. [32] and Richardson et al. [31]. DELORES, for example, is a tool that uses the MCMC approach to generate stochastic occupancy profiles, energy use for appliances and lights, and thermal comfort settings in buildings [34]. The

MCMC concept has recently been applied on the district-scale in Ref. [35] to compare different modeling approaches.

A different approach was used in Ref. [36]. In Switzerland, a building stock modeling tool introduced stochasticity into yearly standard schedules of occupancy from SIA via random *vertical variability* and *horizontal variability*. In the context of that work, vertical variability stands for randomly perturbing each hourly value around its nominal value. Horizontal variability stands for the creation of blocks of hourly periods, and within these blocks shuffling the nominal schedules values with each other [36].

1.2.2. Person-based approaches with single building interactions

Diversity and stochasticity in person-based approaches can be achieved by considering different categories of occupants in buildings. This kind of diversity is usually based on statistical data. For example, for residential buildings in the context of Europe, StROBe [25] has the ability to generate stochastic occupant behavior profiles based on the number of household members and their employment status ('minor', 'full-time employed', 'part-time employed', 'unemployed' or 'retired'). The approach is data-driven, relying on statistical data from TUS, Household Budget Surveys, and Qualitative House Registration Surveys. Another example is SOB by [26] for stochastic behavior modeling of residents in China. For typical households, e.g., 'two office workers, one student, and one retiree', the occupant presence, appliance use, window operation, and air-conditioning (AC) use are modeled by combining different probabilistic models from the literature. Typical household compositions and behavior patterns were based on a large-scale questionnaire survey. Other parameter values were assumed. In [37], various models from the literature are integrated into a room-level stochastic occupancy simulator for office buildings. For a category of occupant, e.g., a 'researcher', arrival and departure events from the office buildings, random movements between different rooms, and meeting events are stochastically generated based on probability distributions and transition probability matrices, which are input data. Such input data could be based on measurements or assumptions.

1.2.3. Person-based approaches with multiple building interactions

Recently, some studies have integrated agent-based urban mobility models with UBEM. In [33], an urban mobility model for Boston based on mobile phone data was used to infer building occupancy. The urban mobility model simulates the daily individual trajectories of 3.54 million people, including

2.10 million 'workers' and 1.44 million 'non-workers' in Boston. Each trajectory consists of a series of stay point coordinates that are characterized as 'home', 'work', or 'other'. The buildings in Boston were classified as 'residential', 'commercial', or 'industrial'. Stay points of people were then probabilistically mapped to buildings to infer building occupancy, whereas 'home' was mapped to 'residential', 'work' was mapped to 'commercial' or 'industrial', and 'other' was mapped to 'commercial'. In an UBEM, this occupancy is then used to simulate energy demands for one representative day in each season for 1266 buildings.

The integration of agent-based urban mobility models and UBEM is promising for applications in existing neighborhoods. However, a space-based, data-driven UBOP might be a suitable and more straightforward alternative for applications in the early design stage of a district. UBOP and urban mobility models could share data sources, instead of full integration of the models.

1.3. Data sources for urban building occupant presence models

Space-based building occupancy models usually require two input parameters, the occupant density and the relative occupancy profiles of buildings. In previous work, it was demonstrated that context-specific occupancy profiles can be created from location-based services (LBS) data [14]. While individual buildings' occupant densities constitute valuable information, it is difficult to obtain them on a large scale due to the limitations associated with determining the absolute number of people from LBS data [10]. An alternative is to obtain data on the total occupancy of a neighbourhood instead of individual buildings. Urban mobility modellers are already extensively relying on such totals in their data-driven models. For example in [38], the absolute number of people performing certain activities in a district was estimated from a combination of public transport passenger data and TUS data. In [39], similar information was obtained from mobile phone data. A data-driven UBOP could use these totals as an input and model the occupant presence in buildings in a way that satisfies the total district occupancy as well as the relative occupancy profiles of buildings. For new developments, the total district occupancy could be approximated by using data of existing districts with similar characteristics.

1.4. Objective and Research Questions

The objective of this work has been to better understand the possible impacts of diversity in commercial building occupancy profiles on simulated district energy demand patterns. Furthermore, the potential impacts on district energy supply systems planning and design decisions have been explored using a case study in the cooling-dominated climate of Singapore. For this purpose, a space-based, data-driven UBOP approach to generate diverse commercial building occupancy patterns has been employed for a high-density, mixed-use, future district of Waterfront Tanjong Pagar. A UBEM tool was then used to simulate end-use energy demand patterns for different choices of UBOP. These demand patterns were then analyzed in relation to the following main research question:

(Q1) How relevant is it to consider diversity in commercial building occupancy profiles for UBEM simulations?

In order to address this high level research question, the following concrete questions regarding the UBEM modeling purpose, the UBOP approach, and the context will be addressed using a case study:

(Q2) What are the impacts of diversity in commercial building occupancy profiles on different phases of the energy system analysis process? (Q3) Is diversity in commercial building occupancy profiles relevant in a district dominated by buildings with regular operational patterns? (Q4) What are the appropriate UBOP modeling approaches for different UBEM simulation purposes and contexts?

In terms of broader impact, urban planners and energy systems planners could make use of this information to choose appropriate UBOP approaches for their context and purpose of UBEM simulation.

To address (Q2), UBEM simulation results of a case study have been produced in sequential order: District occupancy, district demand, renewable energy integration potential, and supply systems design. To address (Q3), the simulation results have been analysed separately for different aggregations of buildings in the district. We considered the aggregation of only commercial buildings in the district and the aggregation of all buildings in the district, including a large share of office and residential buildings with assumed regular operation patterns. To address (Q4), different UBOP have been be developed. They entail a model representing the status-quo and multiple data-driven models. Probabilistic diverse models and deterministic uniform models have been created based on data. Comparing the results of these different UBOP highlights under what circumstances diversity can be neglected and diverse profiles can be substituted with a uniform mean or median profile per building use-type. Such comparisons also provide insight on situations where diversity is highly influential on the results. In these contexts, multiple probabilistic simulations are necessary because single simulation based deductions would present too high levels of uncertainty to be effectively useful.

This paper is organized as follows: Section 2 introduces the methods used for data-driven UBOP, the UBEM tool, and the methods for demand pattern analysis. Section 3 introduces the case study. The results are presented in section 4 in four subsections ordered according to the sequential UBEM simulation results: District occupancy, district demand, renewable energy integration potential, and supply system design. The discussion in section 5 is followed by the assessed limitations in section 6 and the conclusions in section 7. Furthermore, Appendix A details the occupancy modeling and Appendix B urban building energy modeling. Appendix C provides reference comparison of the models to statistical data.

2. Methods

The methods used in this work are comprised of three parts. They are: (1) data-driven urban occupant presence modeling for commercial buildings, (2) urban building energy simulation with a UBEM tool, and (3) the analysis of the district energy potentials and demand patterns. The three parts are introduced in the next sections.

2.1. Data-driven Urban Building Occupant Presence Modeling

The data-driven UBOP in this work is based on location-based services data that serve as a proxy for real measured occupant presence data. In the following sections, the data collection, the occupant presence models, and the relationship of occupancy to internal building loads are described. The methods for data collection and processing are based mainly on previous work in Ref. [14].

2.1.1. Data Collection and Processing

The workflow of [14] was used to collect data in an area of 4km by 4km around the Downtown Core in Singapore, an area immediately adjacent to the proposed development used as the case study. See Fig. 2. *Popular times* data was collected for commercial buildings from Google Maps [40]. Opening hours and place-type information was obtained from the Google Places API [41].

The collected popular times data was categorized into the two use-types, restaurant and retail, based on the place-type information and filtered for seven days of data availability based on the opening hours information. Meaning that places without popular times data during *closed* days were included, and places with missing data during *open* days were excluded. With this procedure, 567 weekly retail occupancy profiles and 1767 weekly restaurant occupancy profiles for the Singapore Downtown and its neighboring areas were obtained. These diverse weekly relative profiles can be directly used as a proxy for measured relative occupancy data in UBEM tools. For example the profiles could be used to replace standard schedules of occupancy.

Figure 2: Data collection site (red) and case study site (green) in Downtown Singapore. Background map from [42].

The occupant behavior model in this work generates the inputs for the UBEM simulation in a two-step process. First, the number of people in each building is determined with a UBOP. Second, occupant-building interactions, such as metabolic heat gains, required ventilation rates, appliance, lights, and hot water use, are calculated based on the number of people in each building. The different UBOP are introduced next.

2.1.2. Occupant Presence Modeling

In total, we compared ten space-based UBOP. See Fig. 3. On the left a baseline model is illustrated (Fig. 3 left) and is based on standard assumptions. On the right nine different data-driven models are shown (Fig. 3 right). All of the models consist of a distinct combination of (a) profiles of relative building occupancy with (b) values of use-type occupant density. District-occupancy *constraints* derived from the baseline, determined the occupant density in the data-driven UBOP.

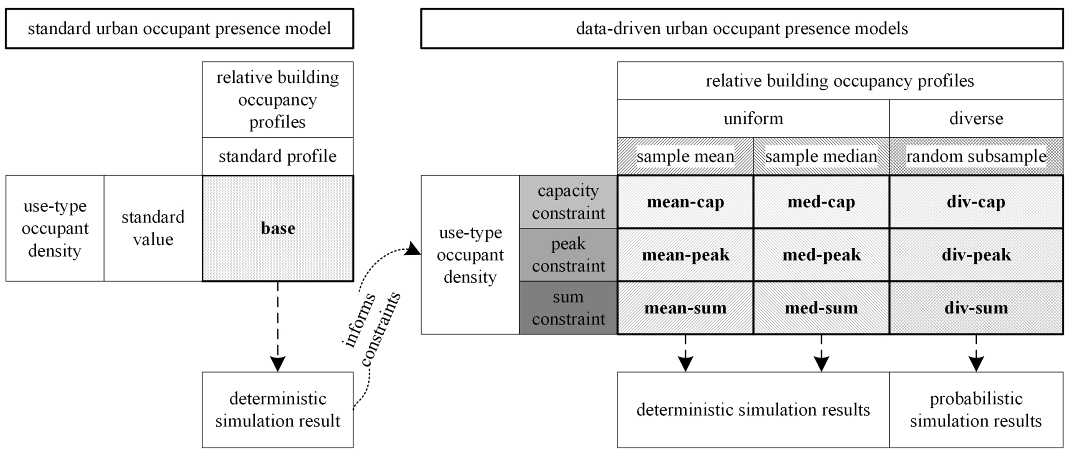

Figure 3: Definition of the different UBOP approaches used in this study. Each model with the standard approach (left) or the data-driven approach (right) consists of a combination of occupancy profile assignment and occupant density parameter values. The occupant density values for the data-driven approaches are based on the constraints derived from the results of the **base** model.

All ten UBOP are defined according to Eq. 1:

$$N_{people,b}(t) = A_{GFA,b}/D_u * p_b(t) \tag{1}$$

where $N_{people,b}(t)$ in $pers.$ is the count of people in building b at hour t of the week, $A_{GFA,b}$ in m^2 is the gross floor area of the building b, D_u in $m^2/pers.$ is the occupant density of the building use-type u, and $p_b(t)$ in % is the relative occupancy of the building b at hour t of the week. Each relative occupancy profile $\mathbf{p_b} = (p_b(1) \ldots p_b(t) \ldots p_b(168))$ is one week long and consists of 168 hourly values in %.

Next, the reasoning leading to ten different UBOP and the terminology used to describe the models is introduced here. The **base** model was based on standard assumptions for profiles and occupant density by ASHRAE [12]. It serves as a baseline throughout this work to which all UBEM simulation results were compared. Details and parameter values are provided in Appendix

A.

We compare different categories of data-driven UBOP: One category with diversity in building occupancy profiles, and another category with single, *non-diverse* or *uniform* profiles. The models with diversity were using randomly chosen subsamples of profiles from the collected data sample. Individual profiles were applied to each of the buildings belonging to the use-type. For the non-diverse models, we considered the hourly mean or the median of the entire data sample as single profile in accordance with research question (Q4). This single profile was then applied uniformly to all buildings of the use-type.

The main departure point of this work was based on the observation that only using standard occupant densities for data-driven UBOP would provide limited insight into the paper's primary research question, which aims to better characterize building to district interaction. The standard assumptions of the **base** model provide a package consisting of temporal relative occupancy profile and occupant density at full occupancy (or design conditions) resulting in the number of people present in all buildings in the district. To compare data-driven UBOP to the **base** model, we propose three mutually exclusive assumptions in line with the considerations introduced in section 1.3. First, we assume that the ASHRAE default occupant densities are good estimates for full occupancy in individual buildings. Second, the ASHRAE standard assumptions are good estimates for the district peak occupancy, which is the maximum hourly count of people during the week within a group of buildings. Third, the ASHRAE standard assumptions are good estimates for the cumulative district occupancy, which is the sum of hourly people counts of the week within a group of buildings.

Additionally, all three assumptions presented are relevant because they highlight varied aspects of district occupancy of interest to different stakeholders involved in building and district planning.

The three assumptions in this work have been translated into modeling *constraints* that can be fixed as an anchor at the district-level. These constraints can be met either by scaling the occupant density or by scaling the relative occupancy profiles. Since the occupancy profiles and their diversity are the focus of this work, the occupant density was treated as a variable.

The **cap** (capacity) constraint fixes the total space capacity (the full occupancy values) of all buildings in the district belonging to one use-type

Cap_u in $pers.$. See Eq. 2:

$$Cap_u = \sum_{b=1}^{B_u} A_{GFA,b}/D_u * 100\% = Const. \quad (2)$$

where $b \in \{1 \dots B_u\}$ are the buildings in the use-type u. The **cap** constraint is straightforward to meet and does not require adjustments of the occupant density because it is independent of the buildings' relative occupancy profile.

The **peak** constraint fixes the weekly maximum hourly count of all people in all buildings of a certain use-type $Peak_u$ in $pers$. See Eq. 3.

$$Peak_u = \max_{1 \leq t \leq 168} \sum_{b=1}^{B_u} A_{GFA,b}/D_u * p_b(t) = Const. \quad (3)$$

where $t \in \{1 \dots 168\}$ are all hourly time steps in a week. The **peak** constraint requires scaling the occupant density of the use-type depending on the relative occupancy profiles.

The **sum** constraint fixes the weekly sum of hourly counts of all people in all buildings of a certain use-type Sum_u in $pers$. See Eq. 4.

$$Sum_u = \sum_{t=1}^{168} \sum_{b=1}^{B_u} A_{GFA,b}/D_u * p_b(t) = Const. \quad (4)$$

The **sum** constraint requires scaling the occupant density of the use-type depending on the relative occupancy profiles. The **peak** and **sum** constraint can be met with one iteration of scaling occupant density. After relative profiles are assigned to each building with an initial guess for occupant density, the number of people in each building can be recalculated using a linear scaling factor so that the chosen constraint is met.

Resulting from the combinations of profiles and constraints, we considered nine data-driven UBOP in this work in addition to the **base** model. Each model is named according to its combination of profile and constraint. See Fig. 3.

Three data-driven **div** (diverse) models were created and consist of random subsamples of context-specific profiles in combination with the three constraints. These models are referenced as **div-cap**, **div-peak**, and **div-sum** according to the specific constraint they meet.

In addition, six uniform data-driven models were created and consist of the combinations of the **mean** and **med** (median) profiles with the three constraints. These models are referenced as **mean-cap**, **mean-peak**, **mean-sum**, **med-cap**, **med-peak**, and **med-sum** according to their combination of profile and constraint.

All **div** models are probabilistic because of the random choice of profiles from the collected data. Each of these three models can be executed N times so that N probabilistic UBEM simulation results are generated that can be statistically analyzed. The single profile **base**, **mean**, and **med** models generate one deterministic simulation result each. The values of the constraints are derived from the results of the **base** model.

In the next section, the models for relationships between occupant presence in buildings and energy-related occupant behavior are introduced.

2.1.3. Occupant-building-interaction modeling

The second step of the occupant behavior model calculates the passive and active energy-related interactions of occupants with buildings required for the UBEM simulations. Occupants interact with the building systems in various ways. The extent of these interactions depends on the building use-type. While residents control almost all systems in their houses, retail customers' interactions with the building are mostly passive. Which of those interactions can be considered also depends on the choice of UBEM (introduced in the next section below).

In our case, occupant behavior is a UBEM simulation input consisting of the following yearly vectors with hourly values: Occupants have metabolic activity. Their presence causes sensible heat gains $\mathbf{Q_s}$ in Wh_{th}/h and latent heat gains $\mathbf{X}$ in g_{water}/h. Occupants' presence also impacts the indoor air quality, which necessitates a fresh air flow rate $\mathbf{Ve}$ in l/s. Their activities in buildings directly or indirectly cause electricity consumption due to the use of lights $\mathbf{E_l}$ in Wh_{el}/h and appliances $\mathbf{E_a}$ in Wh_{el}/h, and the flow rate of hot water $\mathbf{V_{ww}}$ in l/h. Occupants might also impact heating, ventilation, and air-conditioning (HVAC) system operation schedules, in the form of the cooling system set-point temperature $\mathbf{T_{cs}}$ schedule for each hour of the week in $°C$ or the fresh air flow rate.

Our modeling approach for restaurant and retail buildings used rule-based algorithms to calculate the quantities mentioned above from the values of absolute and relative occupancy and the respective nominal values, i.e., the lighting and appliance power density of buildings, and the per-person hourly heat gains, ventilation requirements, and water use. These rule-based algorithms were designed to emulate the implicit relationships between occupant presence and occupant behavior, as presented in the ASHRAE standard schedules [12, 11]. They are described in detail in Appendix A. Noteworthy is the algorithm determining the cooling set-point temperature and the required ventilation flow rate, which was assumed to be presence-controlled. This means that the mechanical ventilation and space cooling systems in commercial buildings are operating during the time when occupants are present (i.e., during the retail and restaurant buildings' opening hours). The required ventilation rate was modeled after a context-specific building code that mandates minimum flow rates per person as well as per area [43]. This results in high $Ve(t)$ even during periods of low occupancy. During zero-occupancy, ventilation systems are switched off, and cooling systems are set-back to a higher temperature of $30°C$. Another point to keep in mind is that in our approach, the electricity consumption for lights and appliances in commercial buildings was not directly related to the absolute number of people in the building. We used only the relative value of occupancy to determine the electricity consumption for lights and appliances. Meaning that changes in occupant density do not influence these electricity demands. All other quantities depend on the absolute number of occupants in the space. See Appendix A. Based on one week of occupant presence generated with the UBOP, yearly vectors of occupant behavior for each building in the district were generated and input into the UBEM simulation.

2.2. Urban Building Energy Modeling

The CityEnergyAnalyst (CEA) tool [2] was used for the UBEM simulations in this work. The CEA is a python open-source urban energy simulation toolbox, including functionality to simulate urban solar radiation, building energy demand forecasting, energy potential assessment, and thermal network and supply systems simulation and optimization. All simulations were carried out with CEA version 2.29 [44]. The next two subsections introduce the building energy demand and solar potential features used in this work.

2.2.1. District Energy Demand

The building energy demand model of the CEA is based on an hourly single-zone resistance-capacitance model based on ISO standards [45]. The solar heat gains of buildings are calculated with the DAYSIM simulation engine [46], which is integrated in CEA. Inputs are the building geometry, defined by the building footprint and the height, the building construction properties, such as the window-to-wall ratio, the window, wall, and roof thermal properties, the building system properties, and the occupant-building-interactions mentioned above in section 2.1.3. The outputs are the hourly end-use energy demands for sensible and latent space heating and cooling, the flow rates and supply and return temperatures of the space heating and cooling systems, the thermal energy demand for water heating, and the electricity consumption of auxiliary systems, such as fans and pumps. The outputs also include the estimated final electricity or fuel consumption of decentralized heating and cooling supply systems.

The typical building and construction properties used in this work were based on context-specific literature and introduced in detail in Appendix B. The weather file used for the simulations is the typical meteorological year for Singapore [47]. A comparison to average energy consumption data in Singapore for all considered building use-types is provided in Appendix C.

From the CEA demand simulation outputs the yearly vectors for each building of hourly thermal demands for space cooling systems $\mathbf{QC_{sys,b}}$ and water heating $\mathbf{Qww_{sys,b}}$ in kWh_{th}/h and the electrical demands for appliances $\mathbf{E_{a,b}}$, lights $\mathbf{E_{l,b}}$, and auxiliary systems $\mathbf{E_{aux,b}}$ in kWh_{el}/h were analyzed. These demands were aggregated when *electric end-use* demands were considered. CEA also converts space cooling and water heating to electric loads $\mathbf{E_{cs,b}}$, $\mathbf{E_{ww,b}}$ in kWh_{el}/h assuming default conversion systems. These outputs were added to electric end-uses when *all-electric*, decentralized building supply systems were considered.

2.2.2. District Solar Potential

The solar potential analysis tool of the CEA [2] was used to calculate the district's renewable energy potential. The inputs into the tool are the selection of pre-defined photovoltaics (PV) technology from the CEA database and the annual radiation threshold in $kWh_{sol}/m^2/yr$ to select roof and facades to install PV panels. The output is the hourly electricity yield from all PV panels installed on the roofs and facades on each building in the district $\mathbf{E_{PV,gen,b}}$ in kWh_{el}/h.

We used a generic monocrystalline PV technology from the CEA database (CEA PV1) with panels installed on every roof and wall surface with annual irradiation of more than 250 $kWh_{sol}/m^2/yr$. The threshold was based on life cycle assessment data and was selected so that the panels receiving this value of annual irradiation are yielding electricity with greenhouse gas (GHG) emission intensity parity with the Singaporean national electricity grid supply mix [48].

The next section introduces the methods for the post-processing of the hourly UBEM simulation results.

2.3. District Demand and Potentials Analysis

The UBOP produces annual hourly district occupancy patterns. The UBEM simulation results deliver the annual hourly energy end-use patterns and annual peak demands. The total all-electric energy demand of all buildings, assuming electric decentralized space cooling and hot water supply systems, is an output of the CEA as well. For the analysis of district occupancy and total energy demand, there was, therefore, no post-processing of the results required. The next two sections introduce the additional metrics calculated to assess the district's potential to integrate on-site renewable energy generation and the metrics used to assess the potential to construct a centralized DCS.

2.3.1. District Renewable Energy Potential Assessment

The potential to integrate decentralized renewable electricity from stochastic sources, such as PV electricity, depends on the expected demand patterns. The *self-consumption* potential determines how much of the generated electricity can be consumed instantaneously on-site. The *self-sufficiency* potential determines how much of the electricity demand can be instantaneously produced on-site.

We used the hourly electricity yield from all the PV panels in the district $\mathbf{E_{PV,gen,district}}$ to calculate the district's solar self-consumption SC_{PV} and self-sufficiency SS_{PV} potentials assuming no storage with Eq. 5 and Eq. 6. We calculated the potential of overall renewable energy share RES_{PV}, assuming perfect storage, in the district with Eq. 7.

$$SC_{PV} = \frac{\sum_{t=1}^{8760} \min(E_{PV,gen,district}(t), E_{D,district}(t))}{\sum_{t=1}^{8760} E_{PV,gen,district}(t)} \tag{5}$$

$$SS_{PV} = \frac{\sum_{t=1}^{8760} \min(E_{PV,gen,district}(t), E_{D,district}(t))}{\sum_{t=1}^{8760} E_{D,district}(t)} \tag{6}$$

$$RES_{PV} = \frac{\sum_{t=1}^{8760} E_{PV,gen,district}(t)}{\sum_{t=1}^{8760} E_{D,district}(t)} \tag{7}$$

where $t \in \{1 \dots 8760\}$ are all hourly time steps in a year and $\mathbf{E_{D,district}}$ is the electrical energy demand considered in the district. We used two different electrical energy demands for the renewable energy potential assessment. The electrical end-use demands were calculated either as $\mathbf{E_{D,el,district}}$ with Eq. 8, or if all-electric decentralized building supply systems were considered, as $\mathbf{E_{D,el,district}}$ with Eq. 9.

$$\mathbf{E_{D,el,district}} = \sum_{b=1}^{B_{district}} \mathbf{E_{a,b}} + \sum_{b=1}^{B_{district}} \mathbf{E_{l,b}} + \sum_{b=1}^{B_{district}} \mathbf{E_{aux,b}} \tag{8}$$

$$\mathbf{E_{D,all,district}} = \mathbf{E_{D,el,district}} + \sum_{b=1}^{B_{district}} \mathbf{E_{cs,b}} + \sum_{b=1}^{B_{district}} \mathbf{E_{ww,b}} \tag{9}$$

where $b \in \{1 \dots B_{district}\}$ are all buildings in the case study district.

2.3.2. Thermal District Supply System Design Metrics

We analyzed the district's thermal cooling demand in order to assess the potential impacts of the different UBOP onto DCS design. We aggregated the thermal space-cooling demand of buildings in the district to create the annual load duration curves. We then analyzed these load duration curves with the design of a hypothetical centralized DCS in mind.

We compared the annual peak demand as a proxy for the investment cost and the annual energy demand as a proxy for the operation costs. We also calculated the *diversity factor* and the *capacity factor* of the space cooling demand. The diversity factor DF_{cool} quantifies the ratio of the aggregated peak demand in the district to the sum of individual peak demands in the buildings [49]. It provides indications on the potential savings on investment costs when considering a DCS as compared to a decentralized supply system. We then sized a hypothetical centralized cooling plant according to the peak demand in the district. The capacity factor CF_{cool} of that plant quantifies the ratio of the energy provided by the system to its supply capacity. It provides indications on whether the installed capacity is underutilized. In [49] the authors minimized the *fluctuation index* $f = 1 - CF_{cool}$ to optimize the building-mix served by a DCS to maximize the plant utilization for a shorter payback period of investment costs. The value of CF_{cool} might also influence the system choice directly. A low capacity factor might cause engineers to propose a DCS design with lower installed cooling generation capacity and a thermal energy storage (TES) instead.

We used Eq. 10 and Eq. 11 to calculate DF_{cool} and CF_{cool} for three options of *connected buildings*. We were considering all commercial podiums connected, all commercial podiums and office towers connected, and all buildings in the district connected in order to address research question (Q3).

$$DF_{cool} = \frac{\max_{1\leq t\leq 8760} \sum_{b=1}^{B_{DCS}} QC_{sys,b}(t)}{\sum_{b=1}^{B_{DCS}} \max_{1\leq t\leq 8760} QC_{sys,b}(t)} \tag{10}$$

where $b \in \{1 \dots B_{DCS}\}$ are all buildings b connected to the DCS and $t \in \{1 \dots 8760\}$ are all hourly time steps in a year.

$$CF_{cool} = \frac{\sum_{t=1}^{8760} \sum_{b=1}^{B_{DCS}} QC_{sys,b}(t)}{\max_{1\leq t\leq 8760} \sum_{b=1}^{B_{DCS}} QC_{sys,b}(t) * 8760h} \tag{11}$$

In the next section, the mixed-use high-density case study district in Singapore is introduced.

3. Case Study

Our case study is a proposed urban re-development in Singapore, neighboring the existing central business district. As part of a future large urban transformation, called the Greater Southern Waterfront, shipping port terminals will be converted into high-density mixed-use urban districts. The overall project comprises around 2000 ha of land [50, 51, 52]. The Waterfront Tanjong Pagar Project at the Future Cities Laboratory (FCL) looked specifically at the re-development of the port's City Terminals. A transdisciplinary team proposed a phasing plan, including 21 precincts, to be developed over the next 50 years [53]. Different precincts have different urban design and follow a phasing strategy based on predicted space demand in Singapore. For our case study, we selected Precinct 1.1, which is planned to be built first and will be the direct extension of Singapore's central business district.

3.1. Urban Geometry and Population

Two sets of planning information were obtained from the design team: A 3D representation of the district, including the footprints of the selected 'tower & podium' block typology, and the design requirements of the district in terms of total GFA, the total population of residents, and the number of office jobs. See Table 1. The geometry was simplified by removing intermediate roof-gardens and other details, such as the setbacks with increasing tower height. In the simplified geometry, all towers were assumed to be straight without setback. The land-use allocation was not provided. Based on the total GFA requirements, the district's population, and the typical occupant density for office buildings in Singapore [54], the building heights were determined. The towers were assumed to be office use or residential use, whereas the podiums were assumed to be commercial (retail and restaurant). Large podiums were split into smaller buildings in order to assign specific occupancy profiles and vary the share between retail and restaurant use flexibly between different urban design scenarios. The final case study geometry consisted of a total of 145 buildings. They were 29 residential towers and 12 office towers with between 17 to 44 floors and 104 podium parts with five floors each. See Fig. 4. The case study's final design characteristics and original design goals are given in Table 1. The overall use-mix in terms of GFA was 63% residential, 21% office, and 16% commercial. The detailed UBEM parameters are provided in Appendix B.

Table 1: Case study characteristics of Precinct 1.1 - comparison of the simplified geometry used in this work and the original design by FCL.

parameter	simplified geometry	original design
total GFA (m^2)	1,333,861	1,333,300
no. jobs ($pers.$)	27,700	27,700
office occupant density ($m^2/pers.$)	10.0[a]	n/a
office GFA (m^2)	277,000	n/a
no. residents ($pers.$)	24,000	24,000
residential GFA (m^2)	845,040[b]	n/a
residential occupant density ($m^2/pers.$)	34.6[c]	n/a
commercial GFA (m^2)	211,821[d]	n/a

[a] 10 ($m^2/pers.$) is the occupant density of the benchmark large office building developed by researchers of the Singapore-Berkeley Building Efficiency and Sustainability in the Tropics (SinBerBEST) program together with the Singaporean Building Construction Authority (BCA) [54].
[b] The residential GFA is the GFA of all remaining towers after 12 office towers with a total of 277,000 (m^2) have been selected via linear optimization.
[c] This is the result of dividing the total GFA of residential towers by the number of residents.
[d] The commercial GFA is the total area of all podiums.

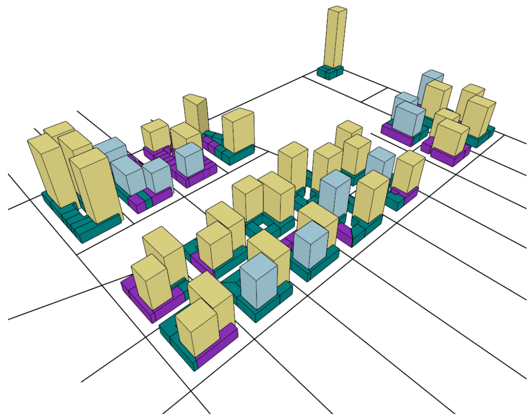

Figure 4: 3D representation of the case study geometry. Retail podium parts are colored in dark green, restaurants in purple. Office towers are light blue and residential towers are khaki.

3.2. Land-use and Occupancy of Commercial Buildings

The case study design did not include the share of use-types in the commercial podiums. For our experiments, we assumed an urban design scenario based on typical Singaporean shopping malls. Due to the increase in online commerce, shopping malls in Singapore are retrofitting to substitute some of the retail space with more food & beverage space. Experts cited in a newspaper article estimate that in the future, restaurants could take up to 40% of the area in malls, as compared to 20–30% in the past [55]. In this work a near-future land-use scenario with 35% restaurant space and 65% retail space was considered. Linear optimization was used to assign commercial podium buildings to the restaurant or retail use-type in a way that matched the desired land-use ratio in terms of GFA.

In this way, 37 buildings were selected as restaurant use-type, and 67 were retail buildings. They are indicated in Fig. 4. In a single **div** UBOP simulation, 37 relative restaurant occupancy profiles and 67 retail profiles were chosen randomly from the collected data (see section 2) to calculate the number of people in each commercial building.

The next section presents the results of the district occupancy and UBEM simulations for the case study with all different UBOP.

4. Results

4.1. District Occupancy

In this section, the cumulative results of the different UBOP on restaurant and retail buildings in the case study are presented first. Then, the impacts on the total district occupancy, including all buildings in the case study, are shown.

4.1.1. Occupancy in Commercial Buildings

Fig. 5 and Fig. 6 show the results of the different UBOP for commercial buildings. The lines in Fig. 5 indicate the number of people in restaurants obtained with the **mean** and **med** models under the three constraints **cap** (a), **peak** (b), **sum** (c). The colored shaded area is the range obtained with the **div** models. The grey shaded area is the number of people obtained with the **base** model. Fig. 6 shows the same information for the retail buildings in the district.

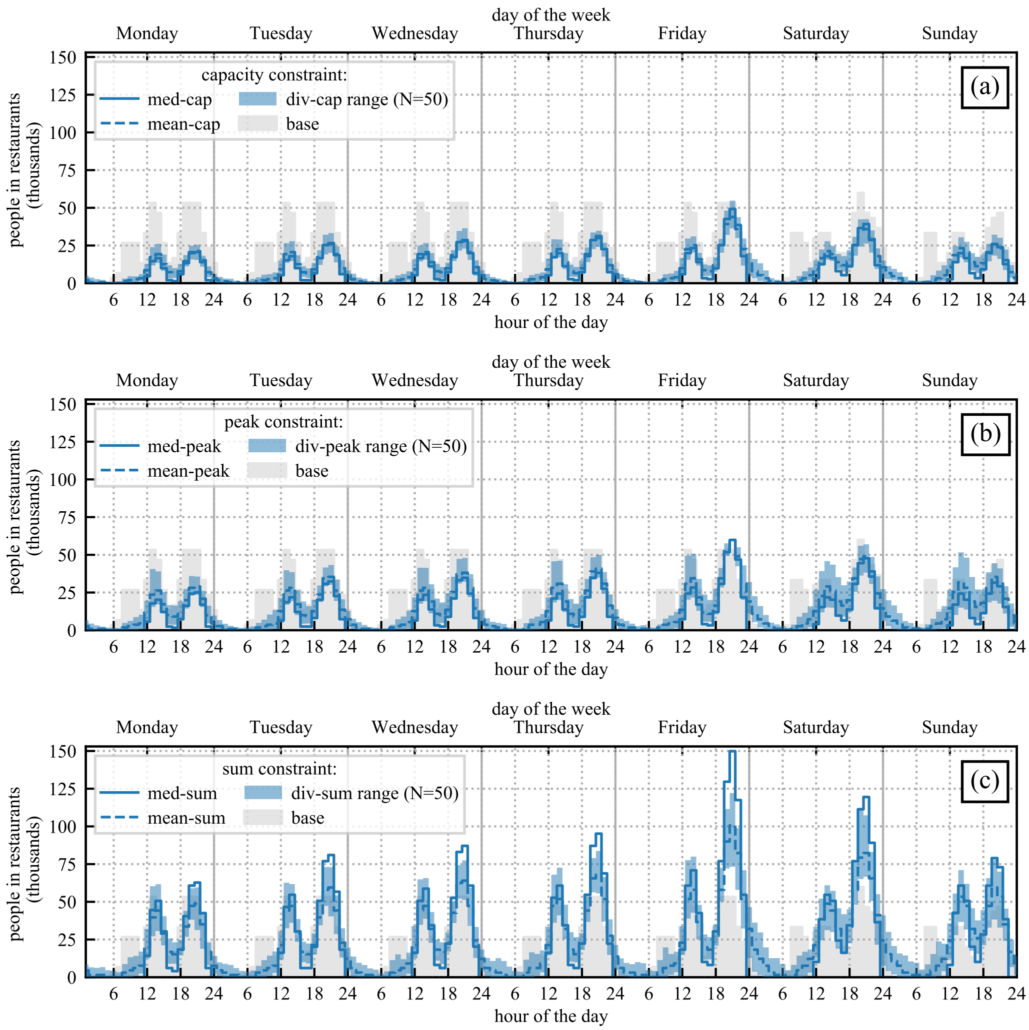

Figure 5: Weekly absolute occupancy in restaurant buildings in the case study district. **mean** and **med** model results are represented by lines. **div** model results (N=50) are given as colored areas between the minimum and maximum of hourly values. The three graphs show approaches under different occupant density constraints: **cap** (a), **peak** (b), and **sum** (c). All graphs contain the **base** occupancy as grey shaded areas.

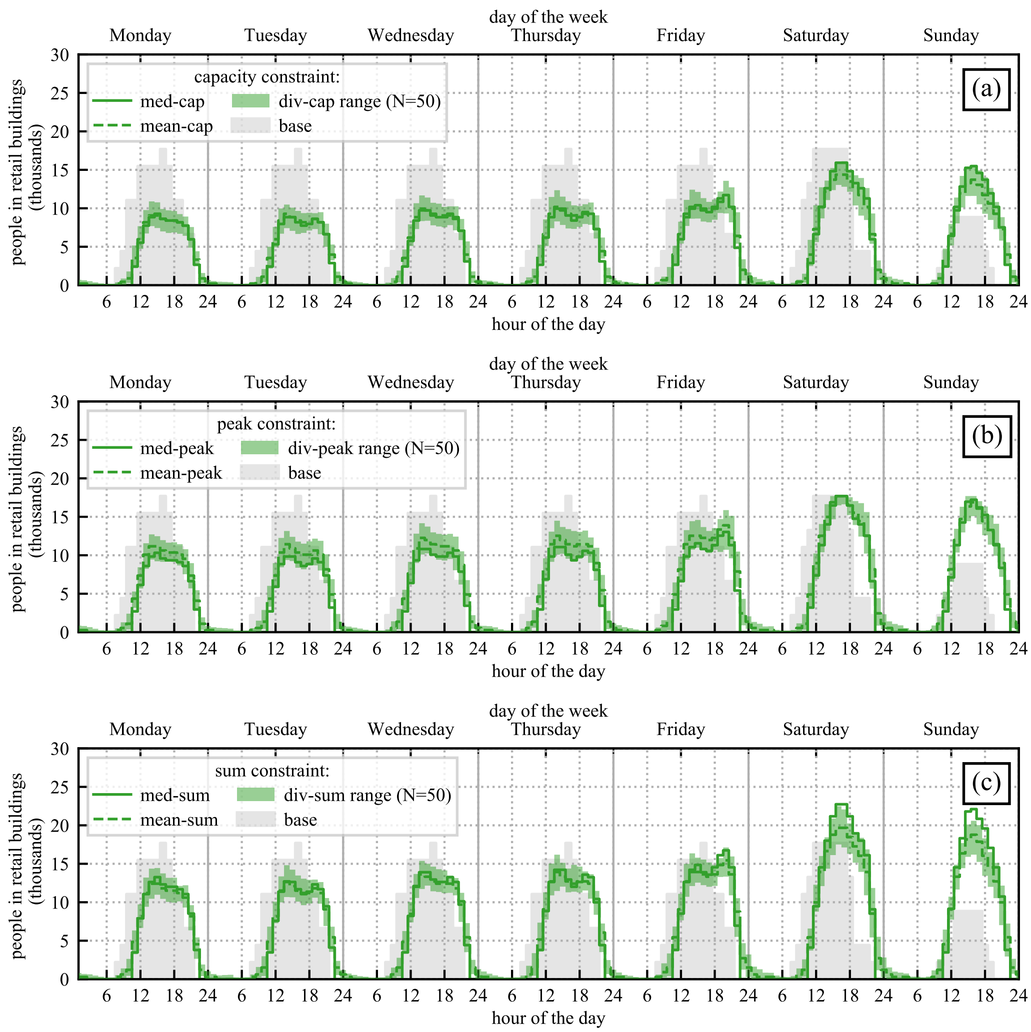

Figure 6: Weekly absolute occupancy in retail buildings in the case study district. **mean** and **med** model results are represented by lines. **div** model results (N=50) are given as colored areas between the minimum and maximum of hourly values. The three graphs show approaches under different occupant density constraints: **cap** (a), **peak** (b), and **sum** (c). All graphs contain the **base** occupancy as grey shaded areas.

Comparing Fig. 5 and Fig. 6 shows that the impact of UBOP choice on restaurants was more pronounced than on retail. While restaurants represent only around 5.5% of the district's land-use, they hosted around 150,000 people in the most extreme case (**med-sum**). Comparing the different models, it can be observed that the **med** were below the **div** results during low occupancy, i.e., in the early morning, the late evening, and in the afternoon valley between the peaks. At the same time the **med-sum** during high occupancy was above the **div-sum**. The **mean** models were in the middle of the **div** range, as expected. The **mean** and **med** occupancy were relatively close. Differences occured mainly at very low occupancy (morning and evening) and during peak hours. For restaurants, the data-driven models' peak occupancy usually occured on Friday night. However, peaks can also be observed at other times, especially under the **peak** constraint. The differences in models for retail buildings are less drastic than for restaurants. The difference in peaks between the different constraints was less than 10,000 people. The data-driven occupancy for retail is generally lower on weekdays and generally higher on Sundays as compared to standard schedules.

4.1.2. Total District Occupancy

Fig. 7 depicts the resulting total weekly district occupancy patterns obtained with the different UBOP. For visualization purposes, only the days from Thursday to Sunday are shown. Monday to Wednesday is identical to Thursday and Friday for the **base** model and similar to Thursday for data-driven models. See Fig. 5 and Fig. 6. The **base** occupancy for the entire district is shown in Fig. 7(a), the data-driven occupancy for the **cap** constraint is shown in Fig. 7(b), (c) shows **peak**, and (d) shows **sum**.

In the **base** model, the regular weekly peak of 93 thousand people occured at 1 PM every weekday from Monday to Friday. When data-driven models were used, the peak was shifted to Friday or Saturday evening. The tallest peak in all models (**med-sum**) was 186 thousand people. The smallest was around 69 thousand people (minimum of **div-cap**).

Fig. 8 shows the district's weekly cumulative occupancy (a) and weekly peak occupancy (b) for all data-driven models relative to the **base**. Deterministic results are indicated with markers. Probabilistic results are presented as boxplots. The whiskers of all boxplots in this paper show the entire range of *div* results of N=50 simulations. The interquartile range is shaded in the graphs to serve as a visual aid.

Models using the **cap** constraint resulted in 24–32% lower cumulative occupancy and 7–26% lower peak occupancy compared to the **base** occupancy. This was due to the overall lower data-driven profiles compared to the standard profiles. See Fig. 5 and Fig. 6. The **peak** constraint resulted in similar peaks compared to the **base**, as expected. However, the cumulative occu-

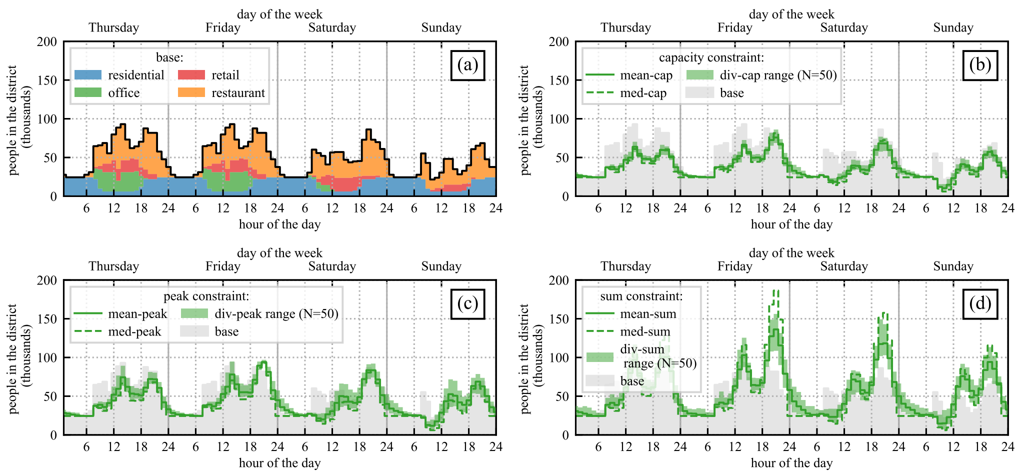

Figure 7: Total district occupancy with different UBOP. The **base**(a) indicates the composition of the district occupancy in terms of building use-types. Data-driven UBOP with different constraints **cap**(b), **peak**(c), and **sum**(d) indicate the range of probabilistic **div** results as colored areas and **mean** and **med** profiles as lines. Graphs (b,c,d) also show the **base** occupancy as shaded area for comparison.

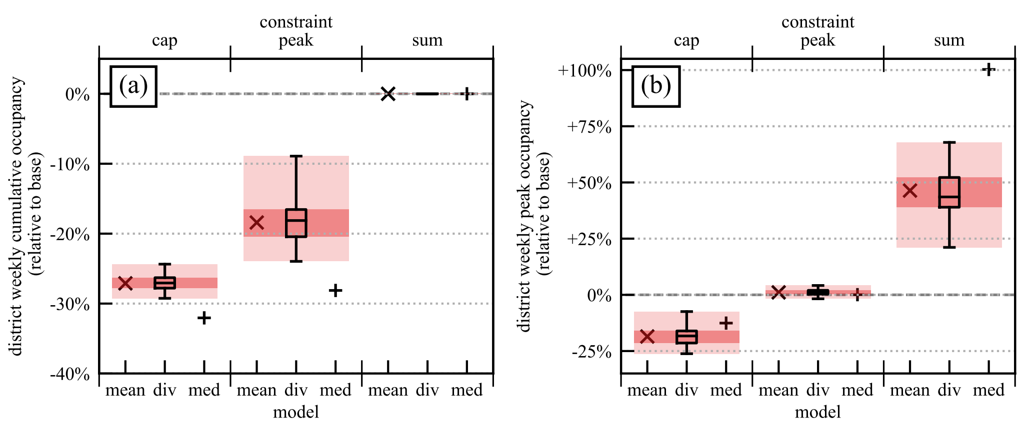

Figure 8: Total district cumulative occupancy (a) and peak occupancy (b) of data-driven UBOP relative to the **base**. The whiskers of the boxplots indicate the minimum and maximum of N=50 *div* simulation results each.

pancy was 9–28% lower. Only models with the **sum** constraint, as intended, matched the sum of the **base**. However, those models resulted in 21–100% higher peaks. The **med-sum** model produced the most pronounced result. For all constraints, the **mean** results were, as expected, in the middle of the interquartile range of the **div** models. The **med** results were below the minimum of cumulative occupancy or above the maximum of peak occupancy in some cases.

4.2. District Energy Demand

In this section, the UBEM energy demand simulation results for commercial buildings in the district are presented first, and the relationship between occupancy and energy demands in commercial buildings are addressed to uncover the modeling mechanisms leading to differences in simulation results. Then, the total energy demand simulation results of the case study for all UBOP, assuming decentralized all-electric supply systems, are presented.

4.2.1. Energy Demand of Commercial Buildings

Fig. 9 shows the annual energy demand (a) and peak demand (b) for the retail buildings in the district. Fig. 10 shows the annual energy demand (a) and peak demand (b) for restaurant buildings in the district.

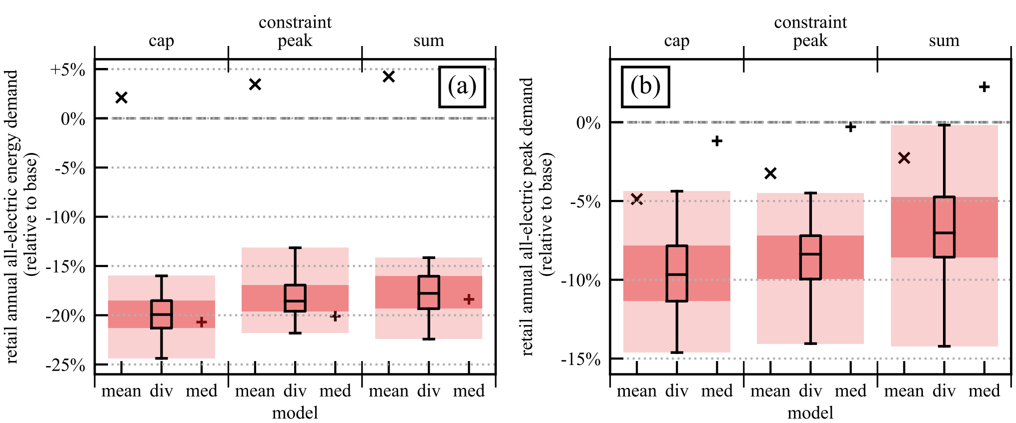

Figure 9: Annual all-electric energy demand (a) and peak demand (b) for all retail buildings in the district obtained with different data-driven UBOP. All results are normalized to the results of the **base** model.

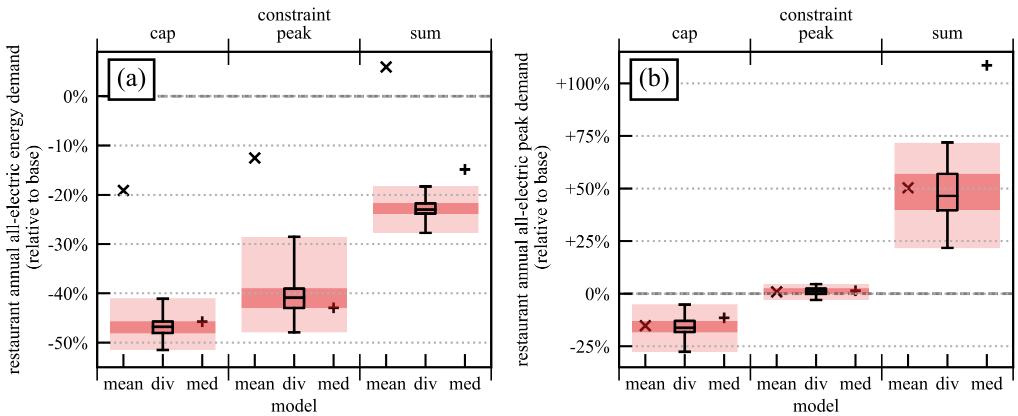

Figure 10: Annual all-electric energy demand (a) and peak demand (b) for all restaurant buildings in the district obtained with different data-driven UBOP. All results are normalized to the results of the **base** model.

Comparing Fig. 9 to Fig. 10 shows that the impacts of UBOP choice on energy demand were more pronounced for restaurants as compared to retail buildings. Aggregated annual demands in retail buildings of **div** and **med** models were 13–24% lower compared to the **base**. **mean** results were 2–4% higher. The peak demand in retail buildings was similar for all models. **div** models resulted in maximum 15% lower peak demands. **mean** and **med** models tended to result in higher peaks compared to the interquartile range of **div** models. Aggregated annual demands in restaurant buildings of **div** and **med** models were 15–51% lower compared to the **base**. **mean** results were above the range of **div** results. At the same time, **mean** results were between 20% lower to 6% higher compared to the **base**. The peak demand in restaurant buildings was highly variable. The data-driven models covered a range of 28% lower to 109% higher compared to the **base** case. The extreme value was obtained with the **med-sum** model, which was also much higher than the **div-sum** results.

To understand this behavior, the 2D histograms of occupancy and energy demand in commercial buildings are presented in Fig. 11 and 12.

Fig. 11 shows the relationship between occupancy in retail buildings and the space cooling energy demand for different models under the **peak** constraint as an example. Fig. 12 shows the same information for restaurant buildings. Colors indicate the frequency of occurrence of specific situations in the district. Please note that the color scale is not linear for better visualization. In Fig. 11 (a), (b), and (c), as compared to the **div** models in (d), it can be observed that models using single uniform profiles frequently generated situations with relatively high cooling demands during relatively low occupancy. This effect was especially pronounced for **mean** models. See Fig. 11 (b). During low district occupancy in **div** models, the people were distributed to few buildings. In contrast, the uniform profiles in the **base**, **mean**, and **med** models distributed a similar total number of people to all buildings in the district. This caused more buildings to operate ventilation and cooling systems and therefore resulted in more space cooling energy demand. The behavior in restaurant buildings was similar. See Fig. 12.

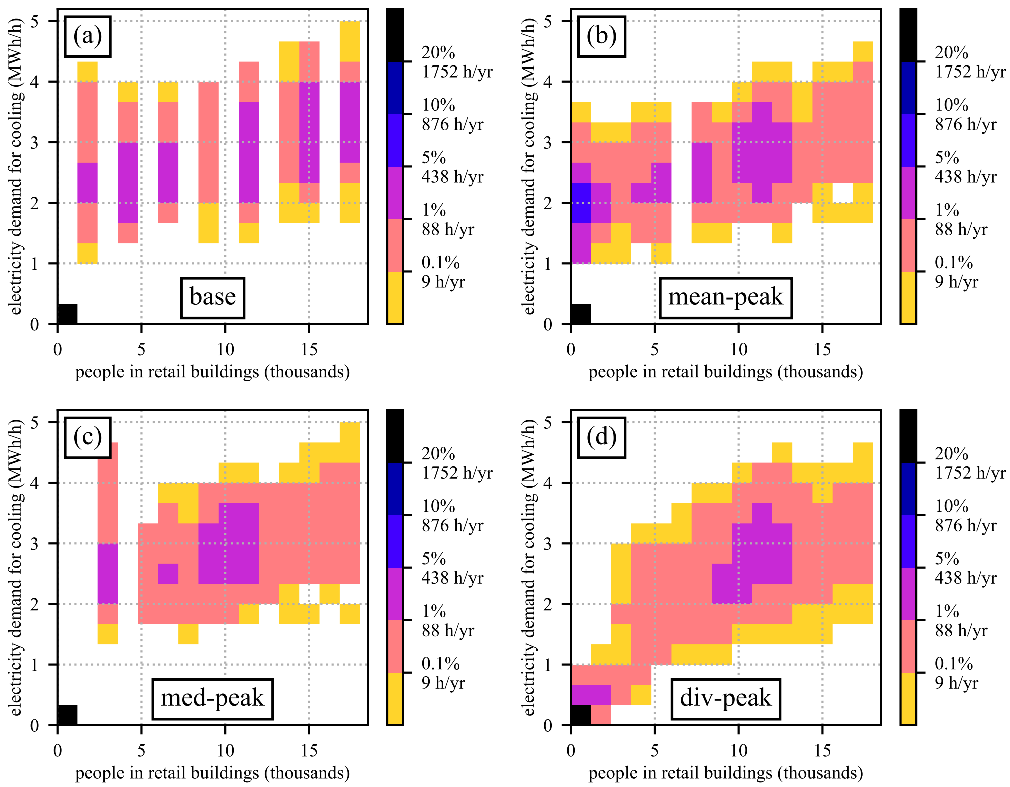

Figure 11: 2D histogram of hourly retail district occupancy (no. of people) vs. hourly space cooling demand in retail buildings. Results of the **base** (a) and the data-driven models under the **peak** constraint are shown. The plots show the **mean-peak** (b), **med-peak**, and the average of N=50 **div-peak** simulations. The colors indicate the frequency of the situations. Please note that the color scale is not linear. One pixel is 1,200 people wide and 0.333 MW high.

4.2.2. Total District Energy Demand

In this section, the impacts of UBOP choice for commercial buildings onto the demand of the entire mixed-use district are presented. In this analysis, all building energy demands of the district, with its predominant office and residential land-use, are aggregated. Fig. 13 shows the annual all-electric, decentralized energy demand (a) and peak demand (b) of the case study district for the different UBOP relative to the **base** occupancy.

The trends in the results were not very different when compared to commercial buildings only (see above). However, the magnitude of differences was

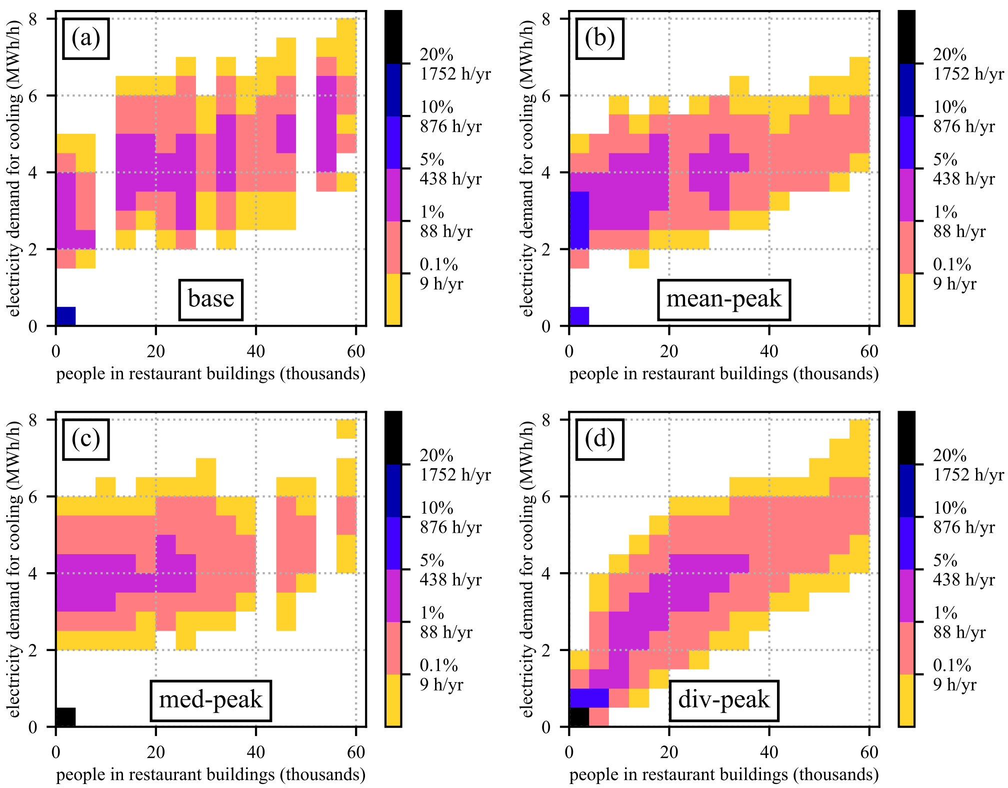

Figure 12: 2D histogram of hourly restaurant district occupancy (no. of people) vs. hourly space cooling demand in restaurant buildings. Results of the **base** (a) and the data-driven models under the **peak** constraint are shown. The plots show the **mean-peak** (b), **med-peak**, and the average of N=50 **div-peak** simulations. The colors indicate the frequency of the situations. Please note that the color scale is not linear. One pixel is 4,000 people wide and 0.5 MW high.

lower. Regarding annual demand, results of **div** models were 8–20% lower compared to the **base**. They were lower even when the **sum** constraint was met. The **mean** results were close (-6% to +3%) to the **base**. However, they were far above the range of results of the **div** models. Regarding the district's peak demand, all data-driven model results were from 14% lower to 13% higher compared to the **base**. **Mean** and **med** results were within the range of the respective **div** models.

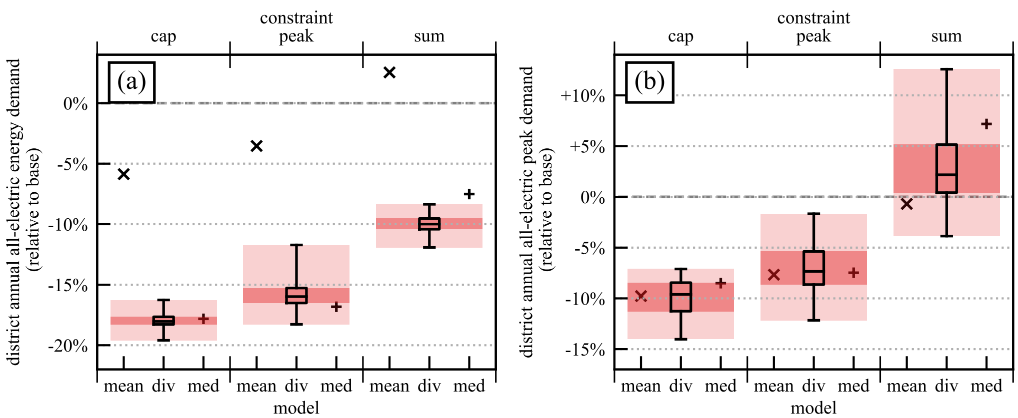

Figure 13: Annual all-electric energy demand (a) and peak demand (b) for the entire district obtained with different data-driven UBOP. All results are normalized to the results of the **base** model.

4.3. District Renewable Energy Potential

In this section, the potential to integrate decentralized renewable electricity generation on the district level is analyzed.

The results obtained with the different UBOP for the overall solar energy share, the solar self-sufficiency, and the self-consumption for two options in terms of demands are compared.

Fig. 14 shows the district's potentials for overall solar energy share (a,b), solar self-sufficiency (c,d), and self-consumption (e,f) obtained with different UBOP. The figure shows two different options in terms of district energy demands considered. The left column (a,c,e) assumes the total all-electric energy demand of the district, including decentralized space cooling and hot water supply systems. The right column (b,d,f) considers only the electric end-use energy demands in the district (appliances, lights, and auxiliary electricity). The results are presented in absolute terms.

For both cases, UBOP approaches with data-driven profiles lead to simulation results that suggest higher renewable energy share, higher self-sufficiency, and lower self-consumption as compared to the **base** standard assumptions. Although the absolute differences were relatively small. While the occupant density and the choice of uniform (**mean, med**) occupancy profile had a considerable impact, the diversity of profiles did not lead to a significant spread in results. In general, compared to probabilistic **div** simulations, the **mean** was underestimating self-sufficiency and overestimating self-consumption. Whereas the **med** models displayed the opposite behavior for self-consumption. However, all results remained in a relatively narrow range. The total spread in data-driven results was never significantly larger than ±1.5%-points. The largest differences between the **base** and data-driven models for any of the metrics did not exceed ±3%-points. The self-consumption was around 96–100%, which can be expected for a district of this density. However, it is important to note that the spread in results of the **div** models was smaller than the difference between **mean** and **med** models. In general, none of the **mean** or **med** model results were within the interquartile range of results of their **div** counterparts.

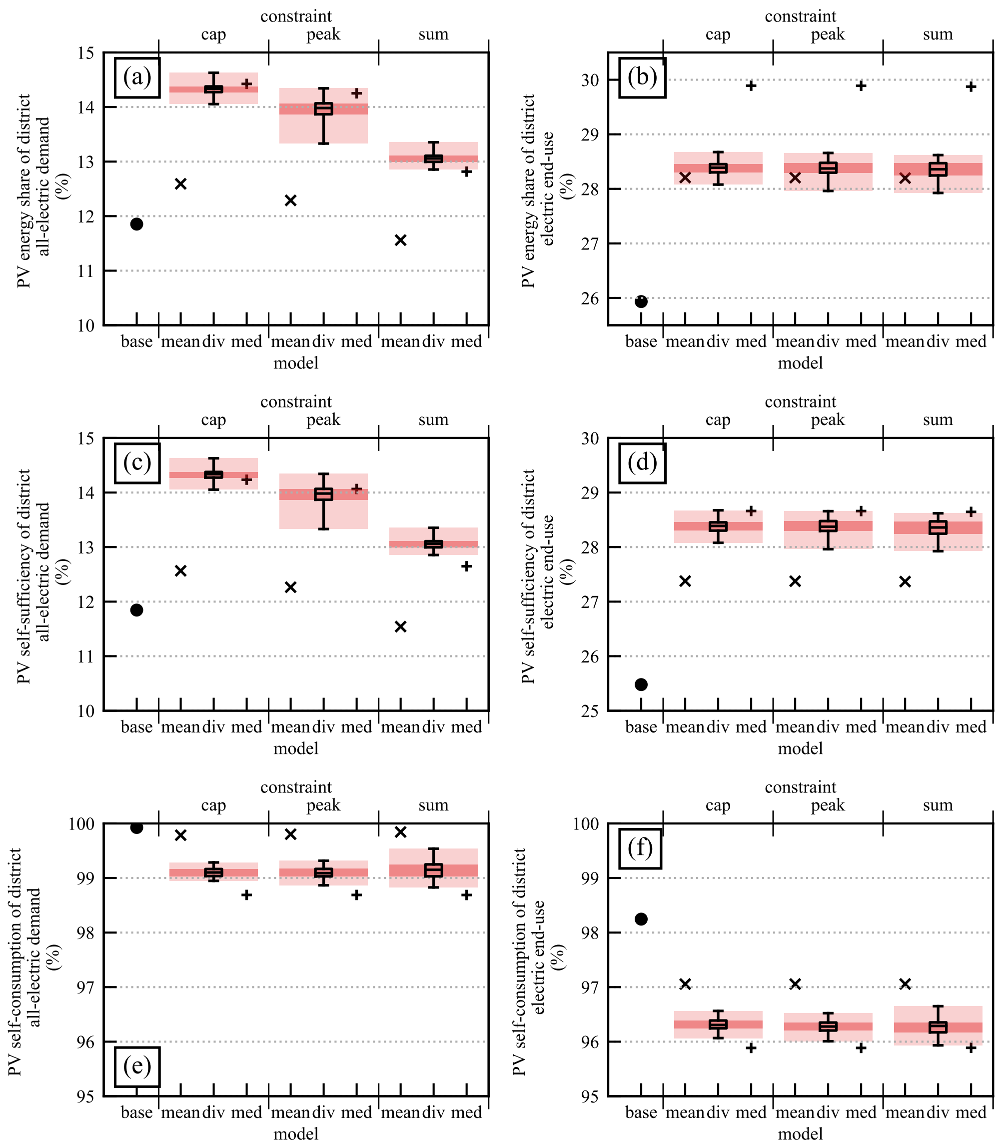

Figure 14: District potential of solar energy share (top row, a, b), district potential of solar self-consumption (middle row, c, d) and solar self-sufficiency (bottom row, e, f), for the case when all demands are converted to electricity (left column, a, c, e) and for the case when only electric end-use energy for lights, appliances, and auxiliary systems is considered (right column, b, d, f).

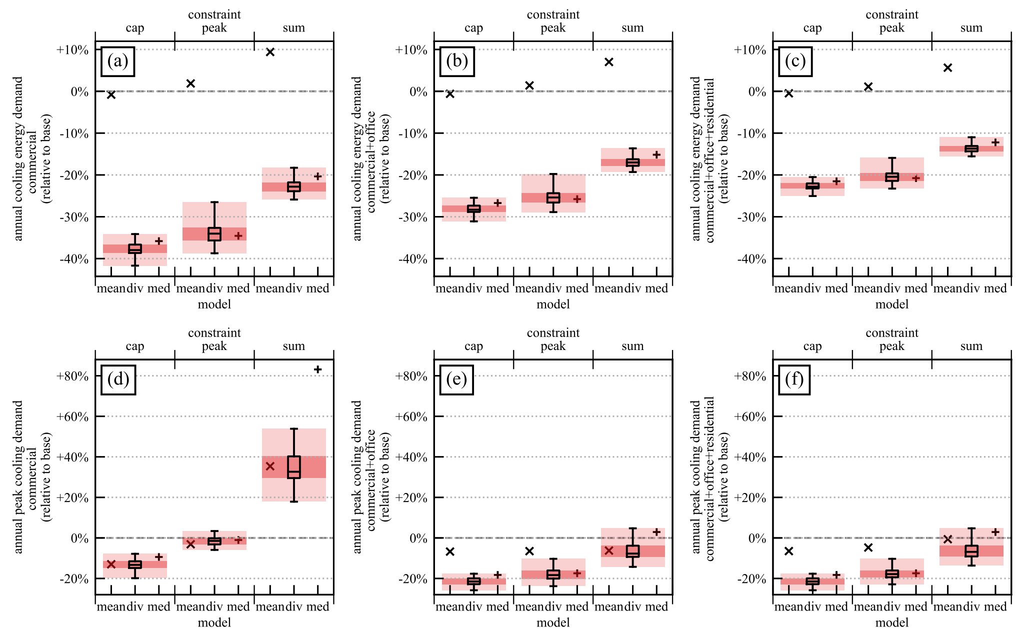

Figure 15: Annual district cooling energy demand (top row, a, b, c) and peak demand (bottom row, c, d, e) with different occupancy models and different combinations of cooling demands. Demands of all commercial buildings (left, a, d), all commercial and office buildings (center, b, e), and all commercial, office, and residential buildings (right, c, f). All values are shown relative to the **base** results.

4.4. Cooling Demand Analysis for District Infrastructure Design

In this section, the district's space cooling demand patterns with respect to the design of a centralized DCS are analyzed. Three options of building interconnections were considered to address the research question (Q3): All commercial buildings are connected to a DCS, all commercial and office buildings are connected, and the entire district (all commercial, office, and residential buildings) is connected.

Fig. 15 shows the annual cooling energy demand (top row) and the annual peak cooling demand (bottom row) for the three options from left (only the commercial buildings are connected) to right (all buildings in the district are connected). The results are presented relative to the results obtained with the **base** model.

From Fig. 15 (d) it can be observed that the peak cooling demand experienced a huge spread when considering only the commercial buildings in the district. The spread reached from -20% to +83% compared to the results of the **base** model. This variation became smaller when all use-types in the district were considered. See Fig. 15 (e, f). One interesting observation is that when commercial buildings' demand patterns were combined with office demand patterns, the **mean-cap** and **mean-peak** models resulted in higher peaks, outside of the range, compared to the respective **div-cap** and **div-peak** results. See Fig. 15 (d, e).

The annual cooling demand was generally smaller than the **base** when modeled with any of the **div** or **med** models. For **div** and **med** models it was -18% to -42% smaller when only commercial buildings were considered and -11% to -25% smaller when all buildings in the district were considered. However, **mean** models resulted in a up to 9% higher annual cooling energy demand compared to the **base**. Also, for the annual energy demand, the differences in results became smaller when more use-types were considered. See Fig. 15 (a, b, c).

Fig. 16 shows the diversity factor (top row) and the capacity factor (bottom row) of the district cooling demand for the three options from left (only the commercial buildings are connected) to right (all buildings in the district are connected). The results are presented in absolute terms. As can be expected, the diversity in commercial building occupancy profiles directly impacted the diversity factor of the space cooling peak demand for commercial buildings in the district. See Fig. 16 (a). The diversity factor was between 59–78% with **div** models compared to around 92–97% with the uniform **base**, **mean**, and **med** models. When more use-types were considered, the diversity factor became smaller, and the range of simulation results became narrower. All non-diverse models, in all cases, resulted in higher diversity factors as compared to the **div** models.

The capacity factor estimation with different UBOP was highly variable when only the commercial buildings in the district were considered. See Fig. 16 (d). **mean** models resulted in higher capacity factors and **med** models in rather lower capacity factors, when compared to the respective probabilistic **div** results. When offices were included in the DCS, the **med** model results fell within the range of **div** results. When office and residential buildings were included, the **base** model and the **div** models produced similar results.

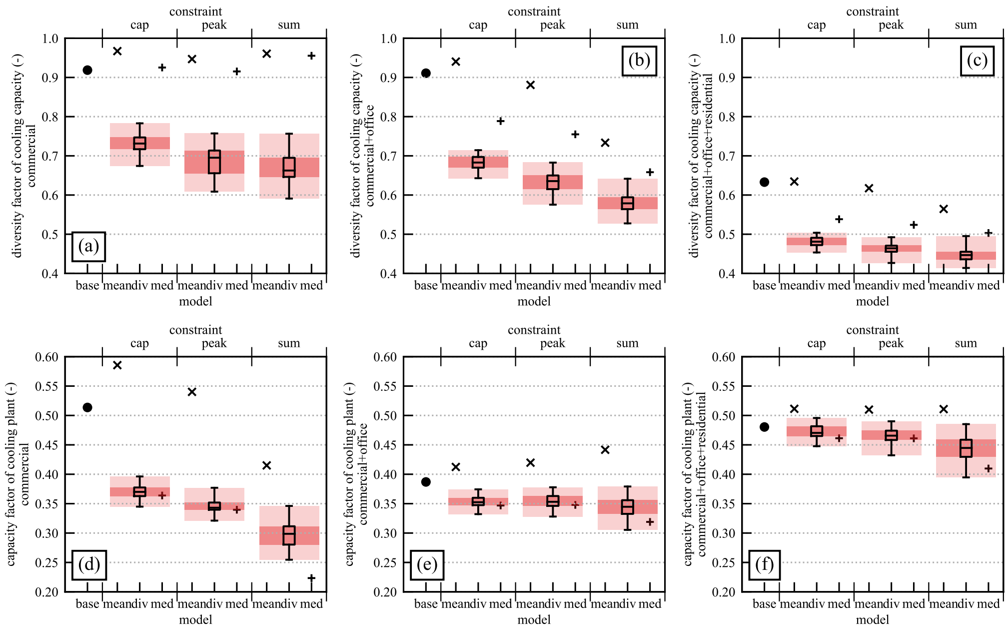

Figure 16: DCS diversity factors (top row, a, b, c) and capacity factors (bottom row, d, e, f) with different UBOP and different combinations of cooling demands: Demands of all commercial buildings (left, a, d), all commercial and office buildings (center, b, e), and all commercial, office, and residential buildings (right, c, f). All values are shown in absolute terms.

In order to better understand these differences in capacity factors, the district's cooling load duration curves are presented here.

Fig. 17 shows the case study district's cumulative load duration curve for space cooling simulated with different occupancy models. The top graph includes the loads of all commercial buildings. The middle graph includes the loads of all office and commercial buildings. The bottom graph includes the loads of all residential, office, and commercial buildings. All load duration curves are presented normalized to the respective peak demand.

The similarity of the different models' load duration curves can be assessed qualitatively in terms of duration. All **div** models generated similar load characteristics. When considering only the commercial buildings in the district, the **mean** results showed the same characteristics compared to the **div** results for around 3000 hours. See Fig. 17(a). The **med** curves were similar to the **div** for around 4500 hours. All uniform UBOP (**base**,**mean**,**med**) were resulting in very different low-load demand patterns compared to the

div models. The **base** and **mean** models generated higher loads for 3000–4000 hours of the year. The **med** models generated lower loads for around 4000 hours of the year.

When all buildings in the district were considered, all models were generating similar thermal load characteristics. See Fig. 17(c).

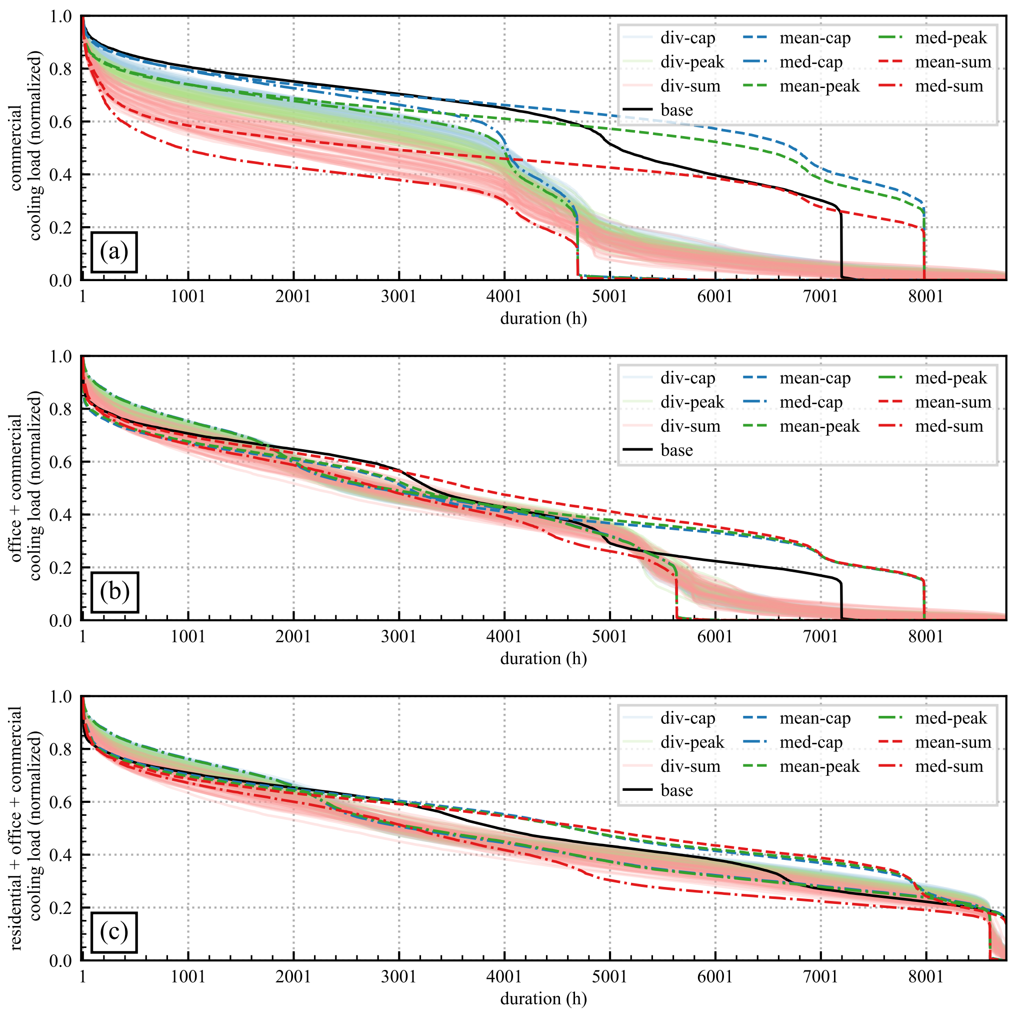

Figure 17: Normalized cooling load duration curves of the case study district for different UBOP and different building aggregations. Graph (a) aggregates the space cooling loads of all commercial buildings. Graph (b) aggregates the loads of all office and commercial buildings. And graph (c) aggregates the loads of all residential, office, and commercial buildings.

5. Discussion

In this section, the results presented above are discussed in the same sequence of district occupancy, demand, energy potentials, and supply systems metrics. At the end of this section, the findings are summarized to answer the research questions.

5.1. Occupant Presence

In general, all UBOP produced expected district occupancy results. The different constraints used for the data-driven models reveal that the occupant density in commercial buildings is a very sensitive parameter for occupant presence prediction. This is not surprising, given that the assumed densities, especially for restaurants, are very high compared to other use-types. Under the **sum** constraint, unrealistically high district occupancy peaks were predicted. The **med-sum** model generated an extreme peak value of more than 186,000 people in the district on Friday evenings, including around 150,000 people in restaurants. We consider this to be unrealistic in relation to the district's residential population of 24,000 people and office-working population of 27,000 people, which will likely have some overlaps. Meaning that the residents of the district might probably will hold some of the office jobs. However, it is not possible to completely rule out one or the other model, because the future district might attract many people from other districts or even tourists from outside the country. This highlights one of the drawbacks of space-based occupancy modeling approaches for UBEM — more buildings (more GFA) automatically 'attract' more people, irrespective of the surrounding context. In this work a way to overcome this limitation by imposing constraints on the number of people on the district-level was proposed. Our data-driven UBOP adjusted the occupant density of buildings according to the selected constraints. In this work, the constraints were based on standard values for occupant density and profiles for comparison. However, it will be difficult to determine realistic values for the constraints for a non-existing development without having access to data from similar, existing neighborhoods in the same context. Such data could be obtained from mobile phone companies that determine the dynamic number of customers in each cell of their network. This kind of data is increasingly used as input for urban mobility models [39].

5.2. Energy Demand

The district energy demand prediction of the UBEM depends on the underlying modeling mechanisms that couple occupant presence to energy demand. In this work, a conservative approach was employed, mimicking as much as possible the implicit relationships between occupant presence and light use, appliance use, water use, fresh air requirements, and cooling setpoint temperatures as found in standards [12, 11, 43] and literature [54]. The observed differences in energy demand of our case study were primarily due to the assumed presence-controlled HVAC systems operation in commercial buildings. This assumption is considered to be valid because, in commercial buildings, occupant presence should correspond to the operating or opening hours. The models based on the **med** profiles provided better estimations for probabilistic results from **div** models. This is likely due to the more realistic building operating hours compared to the **mean** or **base** models. The models based on **mean** profiles generated high demands during low commercial district occupancy because all buildings were occupied and air-conditioned in early mornings and late evenings. Interestingly, these unrealistic building operation patterns generated the only results close to the **base** model. This strong influence of occupant presence and operating hours on space cooling energy demand was most likely a climate-specific effect, related to the year-round need for air-conditioning in Singapore. More research in other contexts could reveal the interplay of different climates and diversity in occupancy profiles on district energy demand. However, this also highlights the importance of realistic occupant-building-interaction models for commercial building use-types in UBEM, such as restaurant and retail buildings. For example, if an HVAC system operation schedule independent of occupant presence was assumed, the results and differences between the models would look very different.

5.3. Energy Potentials

The urban renewable energy potential assessment is related to occupancy via the UBEM demand pattern simulation. The overprediction of the energy demand with **mean** compared to **div** occupancy profiles translated directly to a higher PV self-consumption potential and a lower self-sufficiency. In general, our data-driven UBOP predicted a higher renewable energy share potential from PV compared to the **base** model. This could potentially have implications on electricity supply system considerations and GHG emission benchmarking of districts. However, in our particular case study, due to the high urban density of the district, all UBOP resulted in similar absolute values. Especially because the self-consumption of PV electricity was very close to 100%, the impact of diversity in occupancy profiles is negligible in this case. This could change if districts with lower urban density, for example, suburban districts, or districts with different urban forms and use-mix were modeled.

5.4. Centralized Cooling Supply System Design

The relevant outputs of the UBEM for the design of a centralized DCS were analyzed. The annual space cooling peak demand, the space cooling energy demand, the diversity factor, the capacity factor, and the annual load duration curve serve as indicators for system design decisions, as well as investment and operation costs. The peak cooling demand serves as a proxy for capital investment costs for the district cooling system. It directly impacts the plant size and pipe size. The annual cooling energy demand serves as a proxy for operational cost and GHG emissions of the district system. If only the commercial buildings in our case study are considered, the different data-driven UBOP yielded peak cooling demands in a range of around -20% to +80% compared to the **base** model. At the same time, the cooling energy demand results were in a range of around -40% to +10% compared to the **base**. These are both very large ranges of results, especially considering that usually buildings of similar types are connected in DCS. The spread of energy demand and peak demand among all models became much smaller when the entire district demand was aggregated. It was around 30% (-25% to +5% relative to **base**) for both, the energy demand and the peak demand. This is still considerable, given that the buildings affected by the choice of UBOP constitute only 16% of the GFA in our case study. This trend indicates that diversity withing use-types becomes less significant if the district is highly mixed, meaning that it contains buildings of multiple use-type categories with distinct occupancy and operation profiles. In [56], a DCS for a mixed-use district in Hong Kong was designed based on the cooling load profiles of typical buildings. The chiller plant capacity was sized to be 20% higher than the predicted peak cooling load to account for uncertainties in climate and system design. Later the authors designed the same system under uncertainty using a UBEM with variable parameters for demand prediction [57, 58]. They considered uncertainty in weather, building construction, and internal gain densities (occupant density, equipment and lighting density, and ventilation rate), but not in temporal building occupancy and operation profiles. Their results predicted peak cooling loads of -21% to +9% compared to the reference case. The occupant density and ventilation rate were identified to be the most important variables for annual cooling demand and peak prediction [58]. The range of the peak demand predictions run here is comparable. However, in this study only two parameters (i.e. occupancy profiles and occupant densities) of 16% of the district's GFA were modified. The spread within **div** models under occupant density constraints was around ±5% (**div-cap**) to ±10% (**div-sum**) of the peak demand for the entire district. Meaning that without modifying the most sensitive variables according to [58] and only by shuffling occupancy profiles of a minor use in the district, the uncertainty in peak demand prediction can become as large as the safety factor for chiller plant sizing [56]. This highlights once more the need for UBEM to adequately model the energy demands of commercial buildings in terms of operation and occupant behavior, even if they do not constitute the major use-types in the district. However, the exact land-use mix among commercial buildings, such as restaurants, retail, and other services, will be unknown for green-field and brown-field developments, which adds additional complexity.

The diversity factor of the peak cooling demand is an important metric to argue in favor of or against a DCS. A lower diversity factor translates to higher potential savings in equipment investment costs due to the overall lower capacity requirement. Diversity factors for district cooling system design are often based on the experience of operators. For example, [59, 60, 61] all mention a value of 0.8 based on experience. For a district cooling application in Hong Kong, the diversity factor was determined as 0.81 in a district comprised of 12 building use-types (45% retail GFA) with uniform load profiles [62, 63]. With the presented **div** UBOP, diversity factors were below 0.8 when considering only the two commercial building use-types. This suggests that uniform load profiles for commercial buildings will result in a too high diversity factor estimate. This might ultimately result in decision-makers disregarding the option of a centralized DCS. However, it is important to note that we did not consider any diversity in terms of construction and building system properties. When all four use-types in our case study were considered, the diversity factor reached values of 0.5 and lower with **div** models. Uniform models still predicted higher values in this case, but the **med** models were relatively close to the upper range of **div** results.

The capacity factor relates the annual energy demand to the installed capacity. In [49], the building use-type mix in a district in Hong Kong was optimized to maximize the capacity factor of a DCS plant. Five use-types with uniform load profiles were considered. The maximum achievable capacity factors ranged from 0.4 to 0.45. In the Singapore case study, when only commercial demands were aggregated, the capacity factor results ranged from around 0.2 to 0.6. This range became narrower to 0.4 to 0.5 when office and residential buildings were connected. **Base** and **med** model results were both within the range of **div** results. **mean** models predicted higher values. A broad range of values are interpreted in these models, especially for commercial buildings, as potentially influencing the technology choice for a DCS. A high capacity factor of 0.6 indicates that a system with a large cooling generation capacity (close to the peak demand) will be the appropriate system choice. Whereas, a low capacity factor of 0.2, might shift the decision towards a system consisting of a smaller cooling generation capacity and a TES. The higher capacity factors of **mean** models were caused by the much higher energy demand predictions at part-load conditions. At the same time, the peak demands were comparable to the other models. This can be seen from the differences in the relative load duration curves. These differences in part-load and low-load energy demand will not impact system design decisions based on peak demands. However, DCS design and sizing methods using optimization for plant size and storage size [64] or network [65] might produce significantly different results when one or the other UBOP is used. For this reason, methods that design DCS under uncertainty might be better-suited [57, 58] to be integrated with UBEM.

5.5. Summary

Fig. 18 summarizes the most important case-study-specific results in relation to the stated research questions (Q1–Q4). The range of UBEM results obtained with different data-driven UBOP is provided in the form of a matrix. Columns represent different UBOP and rows represent different UBEM simulation purposes. The values in each cell indicate the range of results relative to the average of **div** simulations (N=50) for a given occupant density constraint.

		RANGE OF UBEM RESULTS (relative to the average of **div** results)								
		cap constraint (lower occ. density)			**peak** constraint			**sum** constraint (higher occ. density)		
UBEM SIMULATION PURPOSE		**div-cap**	**mean-cap**	**med-cap**	**div-peak**	**mean-peak**	**med-peak**	**div-sum**	**mean-sum**	**med-sum**
District energy use / GHG emission benchmarking	Energy demand of retail buildings	<±10%	<±20%	<±10%	<±10%	<±20%	<±10%	<±10%	<±20%	<±10%
	Energy demand of restaurant buildings	<±10%	<±20%	<±10%	<±10%	<±20%	<±10%	<±10%	<±20%	<±10%
	Energy demand of the mixed district	<±10%	<±20%	<±10%	<±10%	<±20%	<±10%	<±10%	<±20%	<±10%
Renewable energy potentials	PV self-sufficiency electric end-use	<±10%	<±10%	<±10%	<±10%	<±10%	<±10%	<±10%	<±10%	<±10%
	PV self-sufficiency for all demands	<±10%	<±20%	<±10%	<±10%	<±20%	<±10%	<±10%	<±20%	<±10%
DCS design	Peak cooling of commercial buildings	<±10%	<±10%	<±10%	<±10%	<±10%	<±10%	<±20%	<±10%	≥±30%
	Peak cooling of the mixed district	<±10%	<±20%	<±10%	<±10%	<±20%	<±10%	<±20%	<±10%	<±20%
	Cooling energy of commercial buildings	<±10%	≥±30%	<±10%	<±20%	≥±30%	<±10%	<±10%	≥±30%	<±10%
	Cooling energy of the mixed district	<±10%	<±30%	<±10%	<±10%	<±30%	<±10%	<±10%	<±30%	<±10%
	Diversity factor of commercial buildings	<±10%	≥±30%	<±30%	<±20%	≥±30%	≥±30%	<±20%	≥±30%	≥±30%
	Diversity factor of the mixed district	<±10%	≥±30%	<±20%	<±10%	≥±30%	<±20%	<±20%	<±30%	<±20%
	Capacity factor of commercial buildings	<±10%	≥±30%	<±10%	<±10%	≥±30%	<±10%	<±20%	≥±30%	<±20%
	Capacity factor of the mixed district	<±10%	<±10%	<±10%	<±10%	<±20%	<±10%	<±20%	<±20%	<±10%

Figure 18: Range of UBEM results for different simulation purposes obtained with three different data-driven UBOP for three occupant density constraints. Columns represent different UBOP and rows represent different UBEM simulation purposes. The values in each cell indicate the range of results relative to the average results of $N = 50$ **div** simulations for a given occupant density constraint. Cells are color-coded according to their value.

Green colored cells represent simulation results within a range of less than ±10% of the respective average of **div** results ($N = 50$). This range was chosen in accordance with the safety factor for DCS plant sizing in [56]. Broader ranges of results fall outside of this safety factor and are indicated with yellow and red colors. The results matrix, for a given occupant density constraint, allows the following three possible interpretations: (a) Diversity in occupancy profiles is not relevant if **div** cells are green and **mean** or **med** cells are green as well. In this case, any of the green models can be used. This also means that probabilistic simulations are not necessary. (b) Diversity is relevant, but probabilistic simulations are not necessary if **div** cells are green and **mean** or **med** are not. And (c) diversity is relevant, and probabilistic simulations should be considered if **div** cells are not green. In this way, we observe that diversity can be relevant for DCS planning purposes. Moreover, especially in high occupant density situations, probabilistic simulations should be considered for DCS design.

It is also observable in Fig. 18 that diversity in profiles tends to be more important when occupant densities are higher (**cap** $<$ **peak** $<$ **sum**). In the same way, it is noticeable that diversity tends to become less important if more building use-types are considered. Furthermore, **mean** occupancy profiles often result in large deviations of energy simulation results when compared to **div** models. This is somewhat counterintuitive, given that the total district occupancy of **mean** models is much closer to average **div** occupancy as compared to the **med** models, as described in section 4.1. This means that in our case study, realistic building operating hours were more important than realistic district occupancy patterns, and therefore mean profiles are not suitable for district energy demand benchmarking. However, this finding is specific to our modeling assumptions of occupant-building-interactions.

6. Limitations

In this study, only the variability of commercial building occupancy profiles due to diversity within two building use-types was considered. Many other factors are contributing to variability in UBEM simulation results. For example, occupant density itself is also a potentially diverse parameter on the building level. Nevertheless, we decided to use one value per use-type. Future studies could treat these parameter values as probabilistic as well. Also, we only considered one option of building systems and controls per use-type. Notably, future buildings might have new types of cooling systems and control systems that could be considered together with different UBOP. Furthermore, we did not consider any variability in the behavior of office occupants and residents. It can be argued that office buildings behave according to more regular schedules and that residential energy consumption in a mixed-use district in Singapore is not dominant. Also, residences will probably not be connected to DCS. Nonetheless, variability in these buildings should be included in future UBOP. We also did not consider variability in climate and weather, and we only considered one exemplary PV technology to assess the renewable energy potential for the district. The uncertainty in climate combined with variability in UBOP might have significant impacts on other renewable energy potentials, such as solar thermal technologies.

7. Conclusion

In this paper, the impacts of UBOP choice onto the simulation results of UBEM were assessed. The main research question was to investigate the relevance of diversity in occupancy profiles among commercial buildings of the same use-type for different UBEM simulation purposes and contexts. To address this question, space-based occupant presence models for retail and restaurant buildings were generated. The baseline (**base**) model represents the status-quo and is based on occupant densities and relative occupancy profiles from ASHRAE [12]. Next, data-driven models with diversity (**div**) and without diversity (**mean**, **med**) in building occupancy profiles were created. Diversity was based on the random choice of weekly profiles based on LBS data from Singapore downtown. For that purpose, popular times profiles from more than 500 retail places and 1700 restaurants from Google Maps [40] were collected.

The models were applied to a case study of a future district in Singapore where retail and restaurant buildings constitute 16% of the total GFA. The two primary building use-types were residential and office. Using the district occupancy of the **base** model as a baseline, we imposed constraints on the data-driven models to keep either the occupant capacity (**cap**), the occupancy **peak**, or the occupancy **sum** constant in the district. The combination of data-driven profiles and constraints produced three diverse probabilistic UBOP and six non-diverse deterministic UBOP.

CEA was used as our UBEM tool to simulate the district's energy demand and PV potential using the ten UBOP. The district energy demand patterns were analyzed to compare relevant metrics for centralized DCS design and operation.

From this case study, several conclusions can be drawn. First in general, occupant density and occupancy profiles are both highly sensitive parameters for district occupancy and district energy demand predictions. Second, the research findings suggests that standard assumptions are conservative. All data-driven UBOP produce lower peaks and lower demands unless the cumulative **sum** of occupants is kept constant, resulting in unrealistic, but not impossible, extreme values of peak occupancy. Third, the interactions between occupant presence and building systems operation are mainly responsible for the differences in energy demand caused by the UBOP choice. In this work, the occupant presence in commercial buildings was assumed to coincide with opening hours and determined the operation patterns of HVAC systems. The major difference between diverse and non-diverse UBOP is the distribution of occupants to buildings in the district. Models with single profiles, such as the **base**, **mean**, and **med** models, generate people in all buildings in the district. In contrast, **div** models with diverse building occupancy profiles can generate a similar total number of people in fewer buildings. This effect was especially pronounced in the **mean** model where periods of very low occupancy resulted in more than 20% higher annual energy demand in commercial buildings compared to **div** and **med** models. This means that GHG emission estimates could be off by 20% just due to the shape of relative occupancy profiles.

Forth, in the considered climatic context, differences in cooling energy demand are mainly responsible for the differences in annual energy demand. The choice of UBOP influences the cooling demand to such a degree that system design decisions might be impacted. The peak cooling demand in the entire case study district was influenced by up to 30% by varying occupant profiles and density in only the commercial buildings (16% of the total GFA). The diversity factor of the cooling load varied in a range that might impact the technology choice and sizing of chillers and TES systems.

Fifth, the PV energy potential assessment results are influenced by the choice of UBOP. However, due to the high demand density in our particular case study, the absolute range of results was not significant.

To summarize, the findings suggest that diversity should be considered for DCS design and probabilistic demand simulations should be conducted for high occupant densities.

8. Outlook

Our results highlight the need for further research on UBOP as well as on building energy modeling of all use-types in cities. Especially retail and restaurant buildings are highly influential on the energy demand and supply in mixed-use districts.

To improve UBOP and to calibrate the very sensitive occupant density parameter, novel data sources could be explored. Such data could come from telco companies that know the temporal patterns of absolute numbers of people in districts.

Furthermore, our results are specific to the climate and case study. Further research on the interplay between occupancy, climate, and urban design is needed. For this purpose, UBEM should consider different building systems and control strategies, and explore uncertainties in construction, building systems, and control parameters together with diversity in occupant behavior.

9. Acknowledgements

This work was developed at the Future Cities Laboratory at the Singapore-ETH Centre, which was established collaboratively between ETH Zurich and Singapore's National Research Foundation (FI 370074016) under its Campus for Research Excellence and Technological Enterprise programme.

Appendix A. Occupant-building Interaction Modeling Details

Occupant-building-interactions are modeled according to ASHRAE standards [12, 11] and context-specific building codes [43] Sensible and latent heat gains as well as ventilation air flow requirements were obtained by multiplication of per-person values with the number of occupants in the buildings. The Singapore Standard 553 also requires a minimum fresh air flow rate per area [43]. The AC systems are assumed to be presence-controlled. See Table A.2 and Table A.3. For the other two use-types in the case study district (office and residential) assumptions and schedules were based on literature and standards. They are introduced as part of Appendix B.

Regarding the relative energy use of lights, appliances, and hot water in commercial buildings, we think that, conceptually, it is important to depict the bandwidth between minimal base load and peak load. Therefore we create rule-based algorithms that can be adjusted without compromising this bandwidth. All algorithms follow the same concept: The minimum load share is fixed according to the minimum observed in the respective standard schedules. The maximum load share is fixed according to the peak defined in the standard schedules. Rules define, when the minimum and maximum occur, based on the current relative value of occupancy, and for water use in restaurants, based on past values of occupancy. For occupancy values in between minimum and maximum consumption, either a linear relationship or a fixed part-load is considered. The algorithms are introduced below in sections Appendix A.1 and Appendix A.2.

Appendix A.1. Restaurant

According to [12] the minimum lighting use in restaurants is 15%, and the maximum is 90% of the installed power density. 15% is observed during zero occupancy. The peak of 90% can be observed for occupancy values $\geq$20%. For our model we implement a simple 3-step control, independent of time of the day and day of the week emulating the general behavior of ASHRAE.

I.e., 15% during no occupancy, 40% during intermediate occupancy, and 90% during peak occupancy. See Alg. 1

Algorithm 1 Relative light power use in restaurants $l(t)$ based on the relative occupancy value $o(t)$.

for all t **do**
  if $o(t) = 0$ **then**
    $l(t) \leftarrow 0.15$ ▷ small consumption when not occupied
  else if $0 < o(t) < 0.2$ **then**
    $l(t) \leftarrow 0.4$ ▷ intermediate consumption during low occupancy
  else if $o(t) \geq 0.2$ **then**
    $l(t) \leftarrow 0.9$ ▷ peak consumption during high occupancy
  end if
end for

According to ASHRAE [12] the minimum appliance use in restaurants is 2% and the maximum is 29%. The schedule is identical for all types of days. The peak of appliance use is reached at 50% occupancy. Between zero and 50% occupancy the relationship is more or less linear. We translate this to our model to Alg. 2

Algorithm 2 Relative appliance use in restaurants $a(t)$ based on the relative occupancy value $o(t)$.

for all t **do**
  if $0 \leq o(t) < 0.5$ **then**
    $a(t) \leftarrow 0.02 + o(t) * 0.27/0.5$ ▷ linear relationship with minimum use
  else if $o(t) \leq 0.5$ **then**
    $a(t) \leftarrow 0.29$ ▷ peak consumption during high occupancy
  end if
end for

According to [11] the water use in restaurants is 0% when the building is not occupied and 15–60% when the building is occupied. The peak is reached twice per day: The first peak occurs immediately after opening during low occupancy, the second peak occurs when 80% occupancy is reached. It seems that a further increase in occupancy does not impact the water consumption (e.g., 90% occupancy on Saturday coincides with 55% water use). During other times the water consumption is more or less linear. We translate this behavior to Alg. 3

Based on the cooling system temperature schedule in [12] the HVAC system operation is approximated with a presence-based set-point, set-back control. The ventilation system provides the minimum fresh air flow rate based on the larger value of the per-person or per-area requirement. During

Algorithm 3 Hourly relative hot water consumption $w(t)$ for restaurant-use based on the hourly relative value of occupancy $o(t)$.

for all t **do**
  if $o(t) = 0$ **then**
    $w(t) \leftarrow 0$ ▷ no consumption when not occupied
  else if $o(t) > 0.0 \land ((o(t-4) = o(t-3) = o(t-2) = o(t-1) = 0) \lor (o(t-4) = o(t-3) = o(t-2) = 0 \land o(t-1) > 0))$ **then**
    $w(t) \leftarrow 0.6$ ▷ peak consumption during first two hours after minimum of 4 hours closing period
  else if $0 < o(t) < 0.8 \land \neg((o(t-4) = o(t-3) = o(t-2) = o(t-1) = 0) \lor (o(t-4) = o(t-3) = o(t-2) = 0 \land o(t-1) > 0))$ **then**
    $w(t) = 0.2 + 0.5 * o(t)$ ▷ linear behavior during off-peak hours
  else if $o(t) \geq 0.8$ **then**
    $w(t) \leftarrow 0.6$ ▷ peak consumption during peak occupancy
  end if
end for

Table A.2: UBEM occupant behavior model parameters for the restaurant use-type.

parameter	value	remarks	source
default occupant density	1.11 $m^2/pers$	average of fast-food and family dining	[12]
ventilation rate	larger value of 5.1 $l/s/pers$ or 3.4 $l/s/m^2$	Singapore standard	[43]
sensible heat gains	80.6 $W/pers$		[12]
latent heat gains	130.1 $g_{water}/h/pers$	calculated from energy value	[12]
cooling set point temperature	$24°C$		[12]
cooling set back temperature	$30°C$		[12]
appliance power density	64.6 W/m^2		[12]
light power density	15.1 W/m^2	ASHRAE Standard 90.1-2016 PRM value	[66]
maximum hot water use	2 $l/pers/h$	calculated from BTU value, assuming water has to be heated by $\Delta T = 50°C$	[11]

zero occupancy the ventilation system is switched off. Table A.2 provides all model parameters for the restaurant use-type.

Appendix A.2. Retail

According to [12] lighting use in retail-use buildings is minimum 5% and maximum 90%. 5% is observed during non-occupied hours. 90% is observed during more than 50% relative occupancy. During off peak hours light-use is somewhere in between. We translate this into a 3-step light control algorithm for retail-use. See Alg. 4.

According to [12] the minimum appliance use in retail buildings is 20%, the maximum is 90%. The peak is reached at 50% relative occupancy. Between zero occupancy and 50% the relationship is relatively linear. We trans-

Algorithm 4 Algorithm to determine relative light use in retail buildings $l(t)$ based on the relative value of occupancy $o(t)$.

for all t **do**
    if $o(t) = 0$ **then**
        $l(t) \leftarrow 0.05$ ▷ light during zero occupancy
    else if $0 < o(t) < 0.5$ **then**
        $l(t) \leftarrow 0.4$ ▷ part load during low occupancy
    else if $o(t) \geq 0.5$ **then**
        $l(t) \leftarrow 0.9$ ▷ peak load during high occupancy
    end if
end for

late this into Alg. 5.

Algorithm 5 Algorithm to determine relative appliance use in retail buildings $a(t)$ based on the relative value of occupancy $o(t)$.

for all t **do**
    if $0 \leq o(t) < 0.5$ **then**
        $a(t) \leftarrow 0.2 + o(t) * 0.7/0.5$ ▷ linear relationship with minimum load
    else if $o(t) \geq 0.5$ **then**
        $a(t) \leftarrow 0.9$ ▷ peak during high occupancy
    end if
end for

According to [11] the minimum water consumption in retail buildings is 4% and the maximum is 62%. The peak consumption is reached at 70% of occupancy. Between zero and 70% the water consumption is relatively linear. We translate these observations into Alg. 6.

Algorithm 6 Rules to determine relative water use in retail buildings $w(t)$ based on the relative value of occupancy $o(t)$.

for all t **do**
    if $0 \leq o(t) < 0.7$ **then**
        $w(t) \leftarrow 0.04 + o(t) * 0.58/0.7$ ▷ linear relationship with minimum use
    else if $o(t) \geq 0.7$ **then**
        $w(t) \leftarrow 0.62$ ▷ peak during high occupancy
    end if
end for

The HVAC systems follow the same control as in the restaurant buildings. Table A.3 provides all model parameters for the retail use-type.

Appendix B. UBEM Modeling Details

Important building energy model parameters used in the UBEM are provided here. They are based on context-specific literature. Office towers

Table A.3: UBEM occupant behavior model parameters for the retail use-type.

parameter	value	remarks	source
default occupant density	6.22 $m^2/pers$		[12]
ventilation rate	larger value of 5.5 $l/s/pers$ or 1.1 $l/s/m^2$ during occupancy	Singapore Standard	[43]
sensible heat gains	73.3 $W/pers$		[12]
latent heat gains	94.6 $g_{water}/h/pers$	calculated from energy value	[12]
cooling set point temperature	$24°C$		[12]
cooling set back temperature	$30°C$		[12]
appliance power density	3.23 W/m^2		[12]
light power density	16.1 W/m^2	ASHRAE Standard 90.1-2016 PRM value	[66]
maximum hot water use	0.7 $l/pers/h$	calculated from BTU value, assuming water has to be heated by $\Delta T = 50°C$	[11]

and commercial podiums (retail and restaurant buildings) share the same construction properties. They are provided in Appendix B.1. The same section also contains the sources of the occupant behavior parameters for office buildings. The model parameters for residential towers are introduced in Appendix B.2. All parameters that are not explicitly mentioned are default parameters in the CEA databases for Singapore as of version 2.29 [44].

Appendix B.1. Office towers building energy modeling parameters

The office building models are inspired by the benchmark model for an energy efficient office in Singapore by [54]. The model was created for Energy Plus, some adjustments for the use in CEA had to be made. The original model is a 20 storey building with a naturally ventilated car park on storey 1-3 and office space on storey 4-20. For this work we did not consider the car park. We also did not consider exterior lighting, facade lighting, and electricity consumption from lifts. Table B.4 provides the construction and systems properties. For the commercial podiums the same construction and system properties as for office towers were assumed. Table B.5 provides the office use-type occupant behavior parameters.

Appendix B.2. Residential towers

Residential tower construction and systems properties are modeled after the Singapore public housing archetype described in [67]. Ranges of typical values for wall and window construction, window-to-wall ratio and light power density are provided. For our model we assume the lowest U-values,

Table B.4: UBEM building model construction and systems properties for office, retail, and restaurant use-type buildings. Most values are based on the SinBerBest benchmark BEM [54].

parameter	value	remarks	source
construction type	CEA T2	medium construction	assumption
envelope leakiness	CEA T1	highly tight, benchmark model has 0.2 ACH at peak time	[54]
roof U-value	0.6 $W/m^2/K$	-	[54]
wall U-value	0.4 $W/m^2/K$	-	[54]
window U-value	2.2 $W/m^2/K$	double glazed on all facades, benchmark model has single glazed windows on south and north facade	[54]
window g-value	0.22	SHGC = g-value, double glazed on all facades, benchmark model has single glazed windows on south and north facade	[54]
WWR	0.59	-	[54]
shading system	CEA T1	-	assumption
HVAC system	CEA T3, CEA T1	central AC and mechanical ventilation with demand control, similar to office Benchmark	[54]
fraction of conditioned GFA	1.0		

Table B.5: UBEM office use-type occupant behavior and system operation parameters.

parameter	value	remarks	source
occupant density	10 $m^2/pers$	used to calculate GFA of case study	[54]
occupancy schedule	benchmark schedule	see Fig. 3 in [54] Appendix	[54]
lights schedules	benchmark schedules	see Fig. 5 and Fig. 6 in [54] Appendix	[54]
lights power density	14.4 W/m^2	composed of office, toilet, and staircase	[54]
appliance schedule	benchmark schedule	see Fig. 7 in [54] Appendix	[54]
appliance power density	14 W/m^2		
HVAC system operation	weekdays 7am - 6pm,Saturdays 7am - 1pm	benchmark model starts at 7.30 with 50% operation, see Fig. 1 and 2 in [54] Appendix	[54]
ventilation rate	larger value of 5.5 $l/s/pers$ or 0.6 $l/s/m^2$		[54]

Table B.6: UBEM building model construction and systems properties for residential use-type buildings.

parameter	value	remarks	source
construction type	CEA T2	medium construction	assumption
envelope leakiness	CEA T3	medium	assumption
Wall U-value	1.2 $W/m^2/K$		[67]
Window U-value	2.2 $W/m^2/K$		[67]
Window g-value	0.22	same window as commercial/office	assumption
fraction of conditioned GFA	0.33	-	[70]
WWR	0.35	average of range in literature	[67]
HVAC system	CEA T2 + CEA T0	mini split-unit and window ventilation	assumption

Table B.7: UBEM residential use-type occupant behavior and system operation parameters.

parameter	value	remarks	source
maximum hot water use	3.1 l/h/pers	standard assumption of 8.6 $l/pers/h$ adjusted to match EUI	[66]
hot water schedule	COMNET Residential	-	[68]
cooling set point	24 C	-	[67]
cooling schedule	ON during the night from 22PM-7AM	every day of the week	[67, 69]
light schedule	ASHRAE schedule D	-	[12]
light power density	1.1 W/m2	initial guess of 2.7 W/m2 [67] adjusted to match EUI	assumption
occupancy schedule	ASHRAE schedule D	-	[12]
occupant sensible heat gain	73.3 W/pers	from ASHRAE BTU value	[12]
occupant latent heat gain	94.6 g-water/pers/h	from ASHRAE BTU value	[12]
appliance schedule	ASHRAE schedule D	-	[12]
occupant density	34.6m2/pers	from case study design, see section 3, very close to ASHRAE value of	
appliance power density	6.2 W/m2	fitted to EUI statistics, ASHRAE value is 6.7 W/m2	assumption
Ventilation rate	0.3 l/s/m2	based on ASHRAE	[12]

projecting some improvement in average future construction. Residential schedules for occupancy, lights, and appliances are taken from [12]. Values and schedules relating to hot water were taken from [68]. The use of AC systems was modeled after the assumptions in [67], which generally agree with the results of a household survey in [69]. The assumptions are: AC use during sleeping, i.e., from 22 PM - 7 AM. The air-conditioned area is 33% of the GFA, based on [70]. We are assuming that in the new district, all residential flats will be equipped with AC systems, which is a conservative overestimation.

Appendix C. Comparison of UBEM EUI to Statistics and Literature

This section aims at adding credibility to the UBEM energy demand simulation. Retail and restaurant buildings are compared to statistical data for energy efficient buildings in Singapore.

Appendix C.1. Retail and Restaurant Building EUI Comparison

Singapore's Building and Construction Authority (BCA) publishes building energy benchmarking reports based on building energy consumption reported by building owners [71]. The published energy use intensity (EUI) data for retail and mixed developments for the year 2018 are provided in Table C.8. There is no specific data available for restaurants.

Table C.8: Reported EUI of retail buildings and mixed developments in Singapore [71].

building type	Top 10% EUI ($kWh/m^2/yr$)	Top Quartile EUI ($kWh/m^2/yr$)	2nd Quartile EUI ($kWh/m^2/yr$)	3rd Quartile EUI ($kWh/m^2/yr$)	Bottom Quartile EUI ($kWh/m^2/yr$)
Large Retail	$\leq$164	$\leq$236	236-422	422-515	>515
Small Retail	$\leq$147	$\leq$238	238-370	370-478	>478
Mixed Development	$\leq$135	$\leq$201	201-269	269-345	>345

Table C.9 provides the average EUI of commercial buildings in the case study obtained with different UBOP. Retail buildings' EUI is in the range of 140-190 $kWh/m^2/yr$, which is in the top quartile of the reported EUI in Table C.8. Restaurant buildings separately are around 360-790 $kWh/m^2/yr$. When the commercial use-mix is considered as a whole, the EUI is in the range of 220-400 $kWh/m^2/yr$. This is within the likely range of large and small retail buildings in Singapore. The BCA report only includes electricity in the EUI values. Gas use in kitchens of restaurants might result in higher EUI in reality in Singapore as reported here. Therefore we consider our UBEM values realistic for energy efficient commercial buildings in Singapore.

Table C.9: Average EUI of retail and restaurant building energy models for different occupancy models.

UBOP	retail EUI($kWh/m^2/yr$)	restaurant EUI($kWh/m^2/yr$)	commercial use-mix EUI($kWh/m^2/yr$)
base	183	742	378
mean-cap	186	600	331
med-cap	145	403	235
div-cap	138-153	360-437	221-248
mean-peak	189	649	350
med-peak	146	424	243
div-peak	143-159	387-531	231-284
mean-sum	190	786	399
med-sum	149	632	318
div-sum	142-158	536-606	283-311

Appendix C.2. Office Towers EUI Comparison

The simulation results for the office towers obtained from CEA match well with the results of the SinBerBest benchmark model [54]. See Table C.10

Table C.10: Comparison of case study office building model to SinBerBest benchmark building model.

demand	CEA model ($kWh/m^2/yr$)	Benchmark model ($kWh/m^2/yr$)	remarks
total EUI	131	131	(excluding carpark, exterior lights, and lifts)
EUI cooling electricity	59	63	
EUI lights and appliances	72	68	
share cooling	46%	47%	

Appendix C.3. Residential EUI Comparison

We estimated the average EUI of residential buildings in Singapore via statistical data of household energy consumption [72], housing type statistics [73], and approximate flat sizes of public [74] and private housing [75]. The EUI of residential towers in Singapore (public and private housing, but excluding landed properties) is roughly 50 - 65 $kWh/m^2/yr$ electricity, plus 6 - 7 $kWh/m^2/yr$ gas (depending on the assumed average flat sizes). The target EUI for our, all-electric residential building model is therefore somewhere between 56 - 72 $kWh/m^2/yr$. The shares of different energy end-uses (cooling, appliances, lights, and hot water) was estimated based on household energy consumption studies in 2012 and 2017 [76, 77]. Table C.11 shows the EUI of residential buildings in the case study district simulated with the CEA.

Table C.11: Comparison of case study residential building model EUI to Singapore statistical data.

demand	CEA building model ($kWh/m^2/yr$)	SG statistical ($kWh/m^2/yr$)	remarks
total EUI electric	64.4	56-72	statistical data incl. gas
EUI lights	3.1	2 - 4	6-4% of electricity consumption
EUI appliances	31.3	20-40 (26-47 incl. gas)	39-61% of electric EUI
EUI water heating	14.2	6 - 14 (only electric)	11 - 21% of electric EUI
EUI cooling	15.8	12-23	24-36% of electric EUI

References

[1] C. F. Reinhart, C. Cerezo Davila, Urban building energy modeling – A review of a nascent field, Building and Environment 97 (2016) 196–202. doi:10.1016/j.buildenv.2015.12.001.

[2] J. A. Fonseca, T.-A. Nguyen, A. Schlueter, F. Marechal, City Energy Analyst (CEA): Integrated framework for analysis and optimization of building energy systems in neighborhoods and city districts, Energy and Buildings 113 (Supplement C) (2016) 202–226. doi:10.1016/j.enbuild.2015.11.055.

[3] Z. Shi, J. A. Fonseca, A. Schlueter, A review of simulation-based urban form generation and optimization for energy-driven urban design, Building and Environment 121 (2017) 119–129. doi:10.1016/j.buildenv.2017.05.006.

[4] F. Domínguez-Muñoz, J. M. Cejudo-López, A. Carrillo-Andrés, Uncertainty in peak cooling load calculations, Energy and Buildings 42 (7) (2010) 1010–1018. doi:10.1016/j.enbuild.2010.01.013.

[5] C. J. Hopfe, J. L. M. Hensen, Uncertainty analysis in building performance simulation for design support, Energy and Buildings 43 (10) (2011) 2798–2805. doi:10.1016/j.enbuild.2011.06.034.

[6] G. Calleja Rodríguez, A. Carrillo Andrés, F. Domínguez Muñoz, J. M. Cejudo López, Y. Zhang, Uncertainties and sensitivity analysis in building energy simulation using macroparameters, Energy and Buildings 67 (2013) 79–87. doi:10.1016/j.enbuild.2013.08.009.

[7] ASHRAE, ASHRAE Handbook—HVAC Systems and Equipment (2016).

[8] L. D. D. Harvey, A Handbook on Low-Energy Buildings and District-Energy Systems: Fundamentals, Techniques and Examples, Routledge, London, UNITED KINGDOM, 2006.

[9] S. Hsieh, N. Schüler, Z. Shi, J. A. Fonseca, F. Maréchal, A. Schlueter, Defining density and land uses under energy performance targets at the early stage of urban planning processes, Energy Procedia 122 (2017) 301–306. doi:10.1016/j.egypro.2017.07.326.

[10] G. Happle, J. A. Fonseca, A. Schlueter, A review on occupant behavior in urban building energy models, Energy and Buildings 174 (2018) 276–292. doi:10.1016/j.enbuild.2018.06.030.

[11] ASHRAE, User's Manual for ANSI/ASHRAE/IESNA Standard 90.1-2004, ASHRAE, 2004.

[12] ASHRAE Project Committee 90.1, Schedules and internal loads for Appendix C, http://sspc901.ashraepcs.org/documents/Addendum_an_Sched_and_Load.pdf (2019).

[13] SIA, SIA 2024 / 2015 D - Raumnutzungsdaten für Energie- und Gebäudetechnik (2015).

[14] G. Happle, J. A. Fonseca, A. Schlueter, Context-specific urban occupancy modeling using location-based services data, Building and Environment (2020) 106803doi:10.1016/j.buildenv.2020.106803.

[15] International Energy Agency, IEA-EBC Annex 66: Definition and Simulation of Occupant Behavior in Buildings, https://annex66.org/ (2019).

[16] International Energy Agency, IEA-EBC Annex 79:Occupant Behaviour-Centric Building Design and Operation, http://annex79.iea-ebc.org/ (2019).

[17] W. O'Brien, S. Gilani, M. Ouf, Advancing Occupant Modeling for Building Design & Code Compliance: Part 1: Introduction, ASHRAE Journal (Feb. 2019).

[18] Y. Shimoda, T. Fujii, T. Morikawa, M. Mizuno, Evaluation on Residential Energy Efficiency Programs Using the City-Scale End-Use Simulation Model, in: Proceedings of 2004 ACEEE Summer Study on Energy Efficiency in Buildings, 2004.

[19] Y. Shimoda, T. Fujii, T. Morikawa, M. Mizuno, Residential end-use energy simulation at city scale, Building and Environment 39 (8) (2004) 959–967. doi:10.1016/j.buildenv.2004.01.020.

[20] Y. Shimoda, T. Asahi, A. Taniguchi, M. Mizuno, Evaluation of city-scale impact of residential energy conservation measures using the detailed end-use simulation model, Energy 32 (9) (2007) 1617–1633. doi:10.1016/j.energy.2007.01.007.

[21] J. Schiefelbein, A. Javadi, M. Lauster, P. Remmen, R. Streblow, D. Müller, Development of a city information model to support data management and analysis of building energy systems within complex city districts, in: Proceedings of International Conference CISBAT 2015 Future Buildings and Districts Sustainability from Nano to Urban Scale, LESO-PB, EPFL, 2015, pp. 949–954.

[22] J. Schiefelbein, M. Diekerhof, A. Javadi, G. Bode, R. Streblow, D. Müller, A. Monti, Development of a Tool Chain For Complex City District Energy System Modeling and Simulation, in: Proceedings of BS2015, Hyderabad, India, 2015.

[23] L. A. Bollinger, R. Evins, HUES: A Holistic Urban Energy Simulation platform for effective model integration, in: Proceedings of International Conference CISBAT 2015 Future Buildings and Districts Sustainability from Nano to Urban Scale, LESO-PB, EPFL, 2015, pp. 841–846.

[24] M. He, T. Lee, S. Taylor, S. K. Firth, K. J. Lomas, Coupling a stochastic occupancy model to EnergyPlus to predict hourly thermal demand of a neighbourhood, in: Proceedings of the 14th International Conference of the International Building Performance Simulation Association (BS2015), International Building Performance Simulation Association (IBPSA), Hyderabad, India, 2015, pp. pp. 2101 – 2108.

[25] R. Baetens, D. Saelens, Modelling uncertainty in district energy simulations by stochastic residential occupant behaviour, Jour-

nal of Building Performance Simulation 9 (4) (2016) 431–447. doi:10.1080/19401493.2015.1070203.

[26] J. An, D. Yan, T. Hong, K. Sun, A novel stochastic modeling method to simulate cooling loads in residential districts, Applied Energy 206 (Supplement C) (2017) 134–149. doi:10.1016/j.apenergy.2017.08.038.

[27] Y. Yamaguchi, Y. Shimoda, M. Mizuno, Development of district energy system simulation model based on detailed energy demand model, in: Proceeding of Eighth International IBPSA Conference, 2003, pp. 1443–1450.

[28] Y. Yamaguchi, Y. Shimoda, T. Asai, M. Mizuno, Development of district energy supply system for CHP implementation, in: Proceedings Of, 2004, pp. 9–121.

[29] Y. Yamaguchi, Y. Shimoda, M. Mizuno, Transition to a sustainable urban energy system from a long-term perspective: Case study in a Japanese business district, Energy and Buildings 39 (1) (2007) 1–12. doi:10.1016/j.enbuild.2006.03.031.

[30] D. Robinson, N. Campbell, W. Gaiser, K. Kabel, A. Le-Mouel, N. Morel, J. Page, S. Stankovic, A. Stone, SUNtool – A new modelling paradigm for simulating and optimising urban sustainability, Solar Energy 81 (9) (2007) 1196–1211. doi:10.1016/j.solener.2007.06.002.

[31] I. Richardson, M. Thomson, D. Infield, A high-resolution domestic building occupancy model for energy demand simulations, Energy and Buildings 40 (8) (2008) 1560–1566. doi:10.1016/j.enbuild.2008.02.006.

[32] J. Page, D. Robinson, N. Morel, J. L. Scartezzini, A generalised stochastic model for the simulation of occupant presence, Energy and Buildings 40 (2) (2008) 83–98. doi:10.1016/j.enbuild.2007.01.018.

[33] E. Barbour, C. C. Davila, S. Gupta, C. Reinhart, J. Kaur, M. C. González, Planning for sustainable cities by estimating building occupancy with mobile phones, Nature Communications 10 (1) (2019) 1–10. doi:10.1038/s41467-019-11685-w.

[34] A. M. Rysanek, R. Choudhary, DELORES – an open-source tool for stochastic prediction of occupant services demand, Journal of Building Performance Simulation 8 (2) (2015) 97–118. doi:10.1080/19401493.2014.888595.

[35] M. Mosteiro-Romero, I. Hischier, J. A. Fonseca, A. Schlueter, Effects of occupancy modeling on district-scale energy demand simulations, (Submitted Manuscript) 41.

[36] D. Wang, J. Landolt, G. Mavromatidis, K. Orehounig, J. Carmeliet, CESAR: A bottom-up building stock modelling tool for Switzerland to address sustainable energy transformation strategies, Energy and Buildings 169 (2018) 9–26. doi:10.1016/j.enbuild.2018.03.020.

[37] Y. Chen, T. Hong, X. Luo, An agent-based stochastic Occupancy Simulator, Building Simulation 11 (1) (2018) 37–49. doi:10.1007/s12273-017-0379-7.

[38] S. A. Ordóñez Medina, A. Erath, Estimating Dynamic Workplace Capacities by Means of Public Transport Smart Card Data and Household Travel Survey in Singapore, Transportation Research Record 2344 (1) (2013) 20–30. doi:10.3141/2344-03.

[39] C. Anda, S. A. Ordonez Medina, P. Fourie, Multi-agent urban transport simulations using OD matrices from mobile phone data, Procedia Computer Science 130 (2018) 803–809. doi:10.1016/j.procs.2018.04.139.

[40] Google, Google Maps, https://www.google.com/maps (2019).

[41] Google, Google Maps Platform | Places API, https://developers.google.com/places/web-service/intro (2020).

[42] Stamen Design, Maps.stamen.com / toner, http://maps.stamen.com/toner/#12/37.7707/-122.3781 (2020).

[43] Singapore Standards Council, SPRING Singapore, Singapore Standard SS 553:2009 - Code of Practice for Air-Conditioning and Mechanical Ventilation in Buildings, 2009, oCLC: 960821621.

[44] J. Fonseca, D. Thomas, B. K. Sreepathi, S. Hsieh, M. Mosteiro-Romero, G. Happle, R. Mok, L. Rogenhofer, J. Hawthorne, F. Khayatian, Z. Shi, B. L. Ong, orenkiwi, T. H, paulneitzel, E. Riegelbauer, A. Elesawy, M. Sulzer, J. A. B. ACOSTA, strusoftsawen, prakharmehta95, VMarty, CityEnergyAnalyst v2.29.0, Zenodo (Jan. 2020). doi:10.5281/zenodo.3625952.

[45] J. A. Fonseca, A. Schlueter, Integrated model for characterization of spatiotemporal building energy consumption patterns in neighborhoods and city districts, Applied Energy 142 (2015) 247–265. doi:10.1016/j.apenergy.2014.12.068.

[46] C. Reinhart, DAYSIM Advanced Daylight Simulation Software, https://daysim.ning.com/ (2020).

[47] Meteotest, Meteronorm 7 (2018).

[48] G. Happle, Z. Shi, S. Hsieh, B. Ong, J. A. Fonseca, A. Schlueter, Identifying carbon emission reduction potentials of BIPV in high-density cities in Southeast Asia, in: Journal of Physics: Conference Series, Vol. 1343, IOP Publishing, Lausanne, Switzerland, 2019, p. 012077, 00000. doi:10.1088/1742-6596/1343/1/012077.

[49] T. T. Chow, A. L. S. Chan, C. L. Song, Building-mix optimization in district cooling system implementation, Applied Energy 77 (1) (2004) 1–13. doi:10.1016/S0306-2619(03)00102-8.

[50] Channel News Asia, NDR 2019: New attractions, housing and office spaces to be developed in Greater Southern Waterfront, https://www.channelnewsasia.com/news/singapore/ndr-2019-greater-southern-waterfront-pulau-brani-sentosa-keppel-11819376 (2019).

[51] Urban Redevelopment Authority, Greater Southern Waterfront, https://www.ura.gov.sg/Corporate/Planning/Draft-Master-Plan-19/Urban-Transformations/Greater-Southern-Waterfront (2019).

[52] Channel News Asia, NDR 2019: PM Lee on redeveloping Singapore's Greater Southern Waterfront (Aug. 2019).

[53] S. Cairns, D. Tunas, Future Cities Laboratory: Indicia 02, Lars Müller Publishers, 2019.

[54] C. Duarte, P. Raftery, S. Schiavon, SinBerBEST Technology Energy Assessment Report (Apr. 2016).

[55] REUTERS, Singapore malls take lead in bumping up food space to counter online hit, https://www.businesstimes.com.sg/real-estate/singapore-malls-take-lead-in-bumping-up-food-space-to-counter-online-hit (Jun. 2017).

[56] W. Gang, S. Wang, D. Gao, F. Xiao, Performance assessment of district cooling systems for a new development district at planning stage, Applied Energy 140 (2015) 33–43. doi:10.1016/j.apenergy.2014.11.014.

[57] W. Gang, S. Wang, G. Augenbroe, F. Xiao, Robust optimal design of district cooling systems and the impacts of uncertainty and reliability, Energy and Buildings 122 (2016) 11–22. doi:10.1016/j.enbuild.2016.04.012.

[58] W. Gang, G. Augenbroe, S. Wang, C. Fan, F. Xiao, An uncertainty-based design optimization method for district cooling systems, Energy 102 (2016) 516–527. doi:10.1016/j.energy.2016.02.107.

[59] H. Shu, L. Duanmu, C. Zhang, Y. Zhu, Study on the decision-making of district cooling and heating systems by means of value engineering, Renewable Energy 35 (9) (2010) 1929–1939. doi:10.1016/j.renene.2010.01.021.

[60] L. Zhen, D. M. Lin, H. W. Shu, S. Jiang, Y. X. Zhu, District cooling and heating with seawater as heat source and sink in Dalian, China, Renewable Energy 32 (15) (2007) 2603–2616. doi:10.1016/j.renene.2006.12.015.

[61] J. D. Chung, S.-J. Moon, Y.-P. Lee, J.-H. Lee, C.-J. Lee, H. Yoo, Feasibility of ice-slurry application to the district cooling system in korea, International Journal of Air-Conditioning and Refrigeration 22 (03) (2014) 1450018. doi:10.1142/S2010132514500187.

[62] T. T. Chow, W. H. Au, R. Yau, V. Cheng, A. Chan, K. F. Fong, Applying district-cooling technology in Hong Kong, Applied Energy 79 (3) (2004) 275–289. doi:10.1016/j.apenergy.2004.01.002.

[63] T. Chow, K. Fong, A. Chan, R. Yau, W. Au, V. Cheng, Energy modelling of district cooling system for new urban development, Energy and Buildings 36 (11) (2004) 1153–1162. doi:10.1016/j.enbuild.2004.04.002.

[64] R. Khir, M. Haouari, Optimization models for a single-plant District Cooling System, European Journal of Operational Research 247 (2) (2015) 648–658. doi:10.1016/j.ejor.2015.05.083.

[65] J. Dorfner, P. Krystallas, M. Durst, T. Massier, District cooling network optimization with redundancy constraints in Singapore, Future Cities and Environment 3 (1) (2017) 1. doi:10.1186/s40984-016-0024-0.

[66] COMNET, Appendix B - Modeling Data, https://www.comnet.org/appendix-b-modeling-data (2019).

[67] K. J. Chua, S. K. Chou, Energy performance of residential buildings in Singapore, Energy 35 (2) (2010) 667–678. doi:10.1016/j.energy.2009.10.039.

[68] COMNET, Appendix C - Schedules, https://www.comnet.org/appendix-c-schedules (2020).

[69] B. Yang, T. Olofsson, A questionnaire survey on sleep environment conditioned by different cooling modes in multistorey residential buildings of Singapore, Indoor and Built Environment 26 (1) (2017) 21–31. doi:10.1177/1420326X15604206.

[70] S. J. Oh, K. C. Ng, K. Thu, W. Chun, K. J. E. Chua, Forecasting long-term electricity demand for cooling of Singapore's buildings incorporating an innovative air-conditioning technology, Energy and Buildings 127 (2016) 183–193. doi:10.1016/j.enbuild.2016.05.073.

[71] Building and Construction Authority, BCA Building Energy Benchmarking Report 2018, Tech. rep., Singapore (2018).

[72] Energy Market Authority of Singapore, Singapore Energy Statistics - Data Tables, https://www.ema.gov.sg/Singapore_Energy_Statistics.aspx (2019).

[73] Singapore Department Of Statistics, Resident Households By Type Of Dwelling, Annual, https://www.tablebuilder.singstat.gov.sg/publicfacing/createDataTable.action?refId=12308 (2019).

[74] Housing & Development Board, Types of Flats - Housing & Development Board (HDB), https://www.hdb.gov.sg/cs/infoweb/residential/buying-a-flat/resale/types-of-flats (2019).

[75] R. Whang, Condos on GLS sites shrinking in size, https://www.straitstimes.com/singapore/housing/condos-on-gls-sites-shrinking-in-size (Nov. 2015).

[76] Energy Efficient Singapore, Household Energy Consumption Profile - Household Consumption Survey 2012, https://www.e2singapore.gov.sg/overview/households/saving-energy-at-home/HEA (2019).

[77] Energy Efficient Singapore, Household Energy Consumption Study 2017, https://www.e2singapore.gov.sg/overview/households/saving-energy-at-home/households-studies (2019).